

# U-Pb geochronologic evidence for the evolution of the Gondwanan margin of the north-central Andes

David M. Chew<sup>†</sup>

Urs Schaltegger

*Department of Mineralogy, University of Geneva, Rue des Maraîchers 13, 1205 Geneva, Switzerland*

Jan Košler

*Department of Earth Science, University of Bergen, Allegaten 41, N-5007 Bergen, Norway*

Martin J. Whitehouse

*Laboratory for Isotope Geology, Swedish Museum of Natural History, S-104 05 Stockholm, Sweden*

Marcus Gutjahr

*Institute for Isotope Geology and Mineral Resources, ETH-Zentrum, Clausiusstrasse 25, CH-8092 Zürich, Switzerland*

Richard A. Spikings

Aleksandar Mišković

*Department of Mineralogy, University of Geneva, Rue des Maraîchers 13, 1205 Geneva, Switzerland*

## ABSTRACT

We investigated the Neoproterozoic–early Paleozoic evolution of the Gondwanan margin of the north-central Andes by employing U-Pb zircon geochronology in the Eastern Cordilleras of Peru and Ecuador using a combination of laser-ablation–inductively coupled plasma–mass spectrometry detrital zircon analysis and dating of syn- and post-tectonic intrusive rocks by thermal ionization mass spectrometry and ion microprobe. The majority of detrital zircon samples exhibits prominent peaks in the ranges 0.45–0.65 Ga and 0.9–1.3 Ga, with minimal older detritus from the Amazonian craton. These data imply that the Famatinian-Pampean and Grenville (= Sunsas) orogenies were available to supply detritus to the Paleozoic sequences of the north-central Andes, and these orogenic belts are interpreted to be either buried underneath the present-day Andean chain or adjacent foreland sediments. There is evidence of a subduction-related magmatic belt (474–442 Ma) in the Eastern Cordillera of Peru and regional orogenic events that pre- and postdate this phase of magmatism. These are confirmed by ion-microprobe dating of

zircon overgrowths from amphibolite-facies schists, which reveals metamorphic events at ca. 478 and ca. 312 Ma and refutes the previously assumed Neoproterozoic age for orogeny in the Peruvian Eastern Cordillera. The presence of an Ordovician magmatic and metamorphic belt in the north-central Andes demonstrates that Famatinian metamorphism and subduction-related magmatism were continuous from Patagonia through northern Argentina to Venezuela. The evolution of this extremely long Ordovician active margin on western Gondwana is very similar to the Taconic orogenic cycle of the eastern margin of Laurentia, and our findings support models that show these two active margins facing each other during the Ordovician.

**Keywords:** Gondwana, Andes, Peru, geochronology, zircon, Paleozoic.

## INTRODUCTION

The Andes represent the locus of continued plate convergence through much of the Phanerozoic. Whereas Andean deformation and magmatism have been extensively studied, the early evolution of much of the proto-Andean margin remains poorly understood. The main reason is because exposures of pre-Andean basement rocks are in many places extremely

limited because they are either obscured by later tectonic events along the convergent margin or buried by the ubiquitous volcanic cover.

This problem is particularly acute in the north-central Andes, where Precambrian basement is not exposed for over 2000 km along strike, from 15°S in Peru to 2°S in Colombia. This corresponds to the distance between the northern extent of the Arequipa-Antofalla basement (Fig. 1), a Proterozoic crustal block that experienced 0.9–1.2 Ga Grenville metamorphism (Loewy et al., 2004; Wasteneys et al., 1995), and the southernmost basement exposures in Colombia, the Proterozoic Garzón inlier (Restrepo-Pace et al., 1997; Cordani et al., 2005). This zone is also characterized by substantial development of Andean foreland sediments to the east, so that the basement geology peripheral to the orogen is not known with any degree of certainty.

However, in the Eastern Cordilleras of Peru and Ecuador, Paleozoic metasedimentary sequences are well exposed. Most of these sequences, including the Marañon Complex in Peru (Fig. 2) and the Isimanchi and Chiguinda Units of the Cordillera Real in Ecuador (Fig. 2), are considered to be autochthonous with respect to the Gondwanan margin (Haerberlin, 2002; Pratt et al., 2005). Hence, their heavy mineral assemblages, and, in particular, their detrital zircon populations, should reveal information regarding their source areas—in

<sup>†</sup>Present address: Department of Geology, Trinity College Dublin, Dublin 2, Ireland; e-mail: chewd@tcd.ie.

this case the Gondwanan margin of the northern Andes. Furthermore, granitic magmas that intrude these sequences can carry inherited zircon, which will also provide source information, particularly with respect to deeper crustal levels that would otherwise be impossible to sample.

The age and number of orogenic episodes in these Paleozoic sequences are poorly constrained, especially in the high-grade metamorphic sequences of the Eastern Cordillera of Peru. It is thus entirely unknown how this region relates to other zones along the proto-Andean margin of Gondwana, where the Paleozoic geological history is significantly better understood (e.g., northern Argentina and Venezuela-Colombia; see Ramos and Aleman, 2000, for a review). However, the metasedimentary rocks of the Peruvian Eastern Cordillera are intruded by several phases of Paleozoic magmatism that can be temporally related to the various regional orogenic episodes. The combination of precise U-Pb zircon geochronology from these intrusive rocks with the provenance information described already thus provides new constraints on both the timing of orogeny and the paleogeography of the Gondwanan margin of the north-central Andes during the Paleozoic.

## REGIONAL GEOLOGY

The Andes of Ecuador can be subdivided into a Western Cordillera, consisting of accreted Late Cretaceous oceanic rocks, and an Eastern Cordillera (the Cordillera Real), which consists of Mesozoic plutons emplaced into probable Paleozoic metamorphic pelites and volcanics (Fig. 2). The southern boundary of the accreted oceanic rocks is marked by the Gulf of Guayaquil (Fig. 2). The metamorphic belts of the Cordillera Real continue into northern Peru (Fig. 2), where there is a marked change in the orientation of the Andean chain at  $\sim 6^\circ\text{S}$ , termed the Huancabamba deflection.

South of the Huancabamba deflection, the Peruvian Andes are composed of a Western Cordillera, consisting of Mesozoic sediments intruded by a Mesozoic arc (the Coastal Batholith) with younger Tertiary volcanics and localized plutons (the Cordillera Blanca), and an Eastern Cordillera, consisting of a sequence of metasedimentary schists and gneisses (the Marañon Complex) intruded chiefly by Carboniferous and Permian-Triassic plutons (Fig. 2). The basement to the Western Cordillera north of  $14^\circ\text{S}$  is unexposed but is believed to represent accreted oceanic material (Polliand et al., 2005, and references therein); south of  $14^\circ\text{S}$ , the Coastal Batholith is intruded into Proterozoic

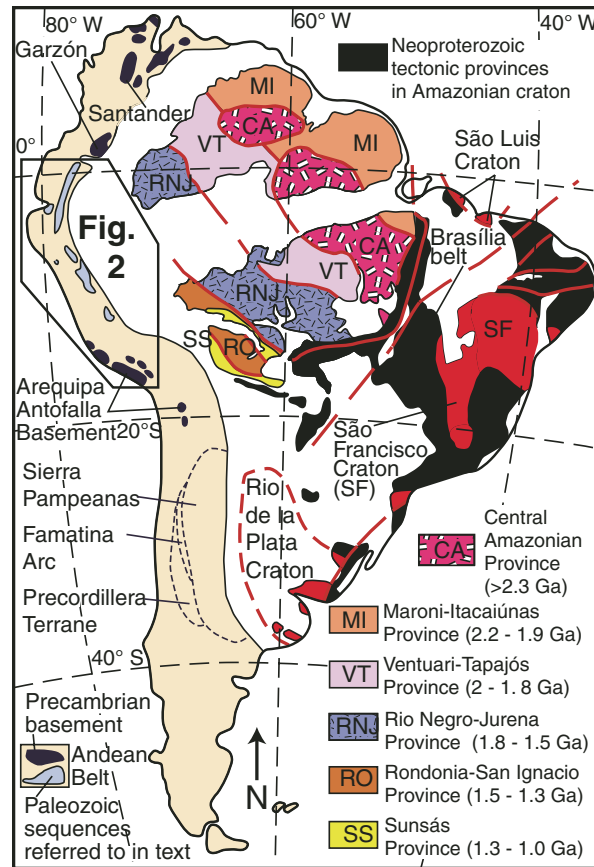


Figure 1. Map of South America illustrating the major tectonic provinces and the ages of their most recent metamorphic events (adapted from Cordani et al., 2000). Precambrian and Paleozoic inliers in the Andean belt are shown in black and light gray, respectively.

gneisses of the Arequipa-Antofalla basement (Figs. 1 and 2).

### Cordillera Real of Ecuador

There is very little age control on the Paleozoic metamorphic pelites and volcanics of the Cordillera Real of Ecuador, and opinion differs as to whether the majority of the units are allochthonous (e.g., Litherland et al., 1994) or autochthonous terranes (e.g., Pratt et al., 2005). The uncertainty relates to the tectonic significance attached to north-south faults that run along the spine of the Cordillera Real. The model of Litherland et al. (1994) invokes these faults as major Mesozoic terrane-bounding sutures that separate a series of suspect terranes. These are illustrated on Figure 2 and are, from west to east: Guamote (continental), Alao (island arc), Loja (continental), Salado (island arc), and Amazonic (continental craton). The model of Pratt et al. (2005) considers these units autochthonous as they share a similar structural history, while the majority of the major terrane-bounding sutures are reinterpreted as intrusive contacts between major plutons and pelites that were reactivated during Andean tectonics. The major phase of fault movement in the region

(which has apparent vertical displacements of many kilometers) is believed to be Miocene-Pliocene in age (Pratt et al., 2005).

### Eastern Cordillera of Peru

Existing age constraints on the timing of deposition and metamorphism of metasedimentary schists and gneisses of the Eastern Cordillera (the Marañon Complex) are very poor. Nd model ages cluster between 1.5 and 2 Ga (Macfarlane, 1999), while a poorly defined Neoproterozoic age has been assigned to the metamorphism based on bulk, unabraded U-Pb zircon data (ca. 630–610 Ma lower intercepts) from granulitic gneisses in central Peru (Dalmayrac et al., 1980). Recent research has demonstrated the presence of an Early Ordovician ( $484 \pm 12$  Ma) metamorphic event in the Marañon Complex (Cardona et al., 2006).

Existing constraints on the timing of magmatism and younger deformation events in the Peruvian Eastern Cordillera are also sparse. However, although based on a very limited geochronological data set (in particular U-Pb zircon), two principal plutonic belts of Paleozoic to Mesozoic age can be distinguished in the Peruvian Eastern Cordillera (Mišković et al., 2005):

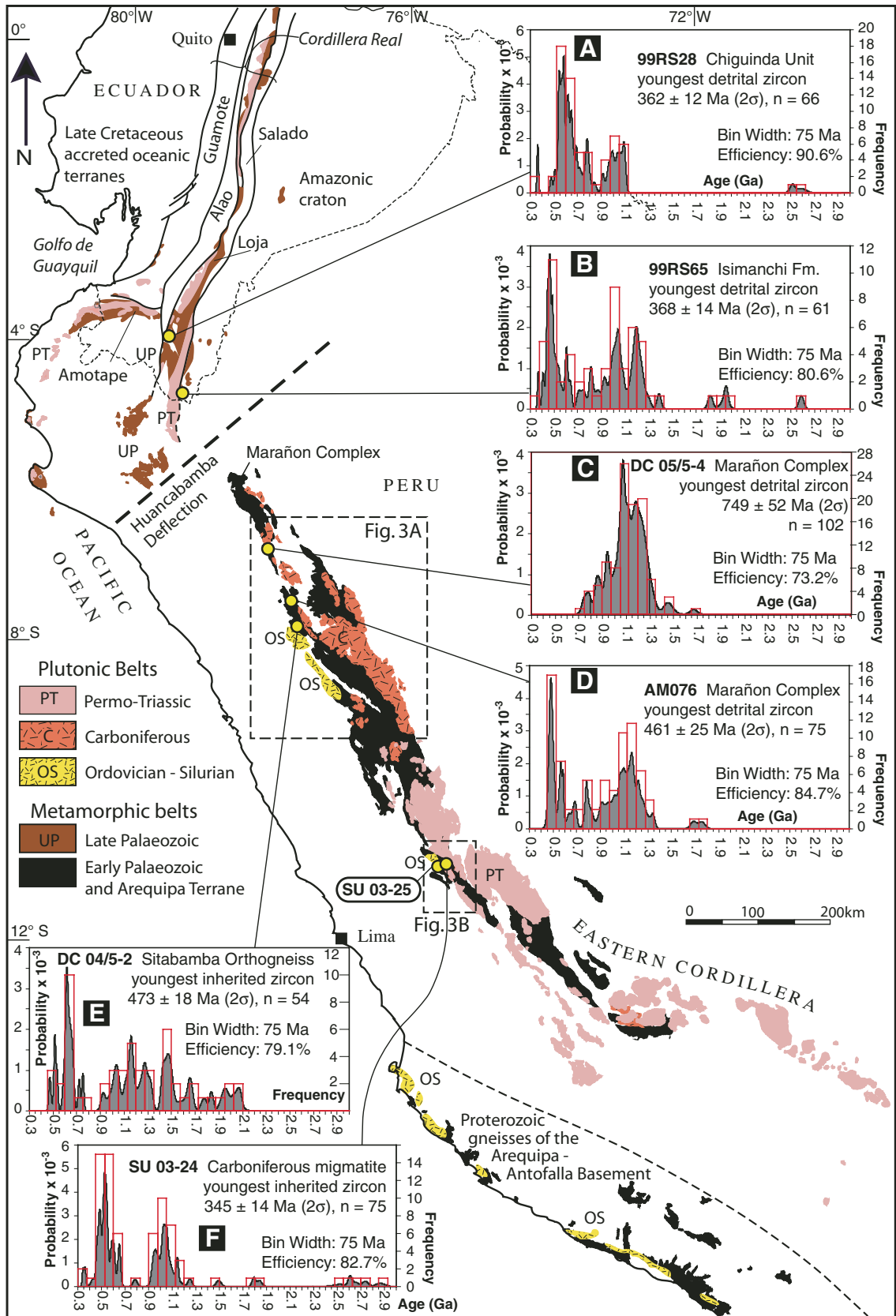
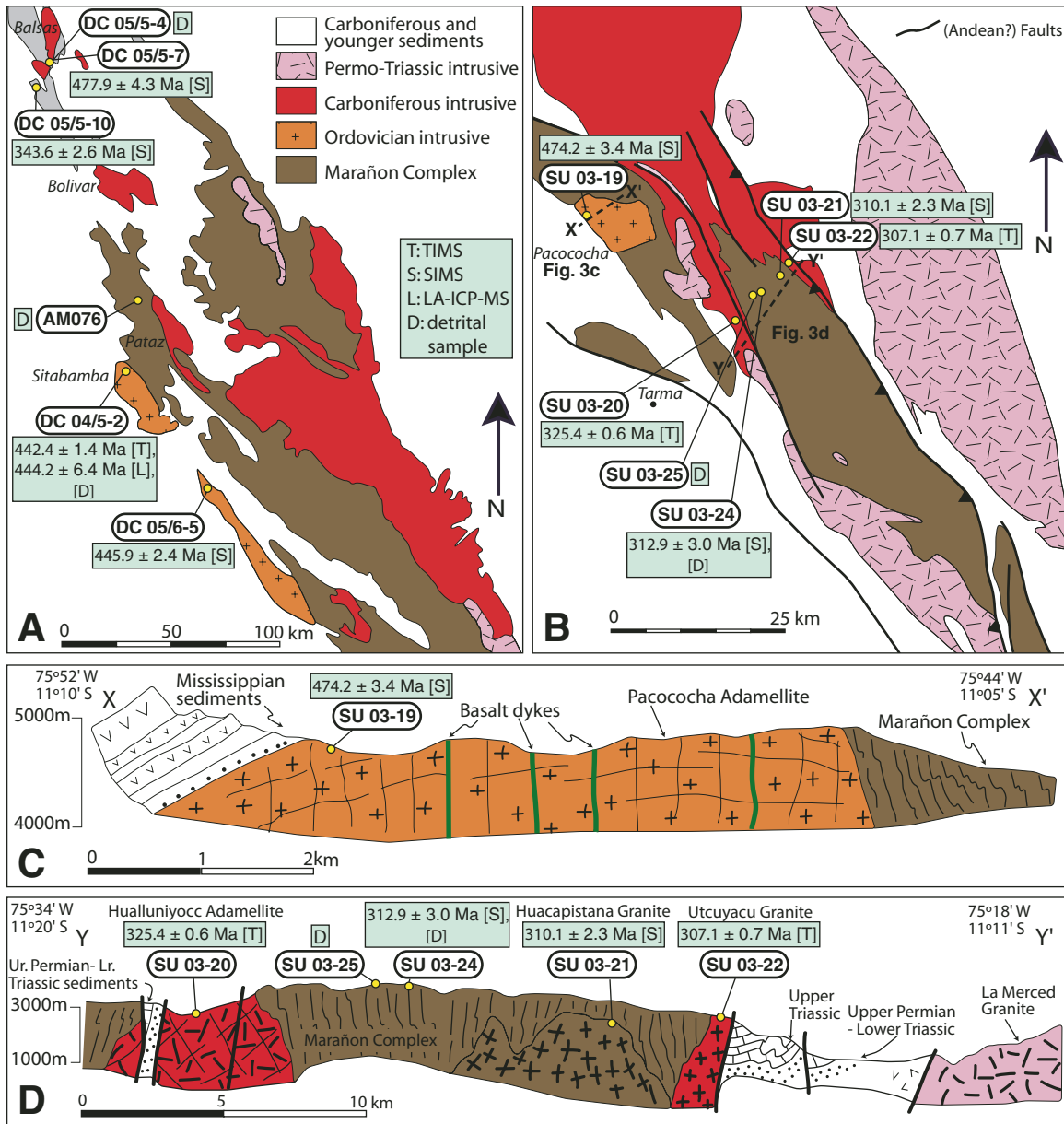


Figure 2. Geological map of Peru and Ecuador illustrating the major Paleozoic metamorphic and magmatic belts along with the Proterozoic gneisses of the Arequipa-Antofalla block. Inset figures A–F illustrate zircon probability density distribution diagrams for both metasedimentary and magmatic (inherited cores) samples. Geology was adapted from Litherland et al. (1994) and Leon et al. (2000).



**Figure 3.** Geological maps, cross sections, and sample localities with ages from selected regions of the Eastern Cordillera of Peru (see Fig. 2). (A) Geological map of the northern section of Eastern Cordillera with names of plutons discussed in the text in italics (adapted from Leon et al., 2000). (B) Geological map of the northern section of Eastern Cordillera (after Mégard, 1978). Legend as in A. (C) Cross-section X-X' through the Pacococha adamellite (after Mégard, 1978). Line of section is indicated in B. (D) Cross-section Y-Y' in the vicinity of Tarma (after Mégard, 1978). Line of section is indicated in B.

Mississippian I-type metaluminous to peraluminous granitoids, chiefly restricted to the segment north of 11°S, and Permian to Early Triassic S- to A-type granitoids in central and southern Peru (Fig. 2). Additionally, the significance and extent of a Late Devonian–Pennsylvanian orogenic cycle (the “Eohercynian orogeny” of Mégard, 1978) remain uncertain. Samples from the Eastern Cordillera of Peru come from two regions (Figs. 2, 3A, and 3B) in northern and central Peru, respectively.

**SAMPLING**

**Ecuador**

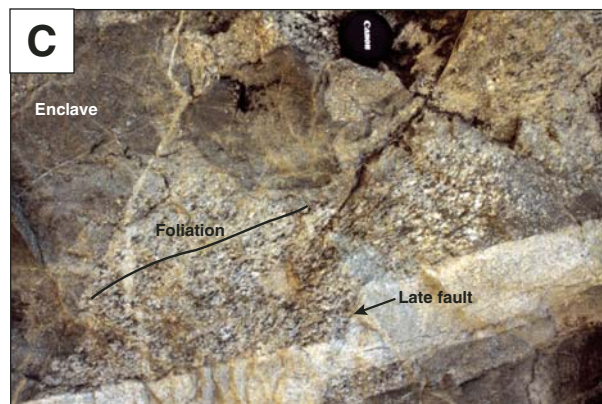
Sample 99RS28 (Fig. 2; grid coordinates for all samples are listed in the relevant data tables in the GSA Data Repository<sup>1</sup>) was selected for detrital U-Pb age zircon analysis by laser-ablation–inductively coupled plasma–mass spectrometry (LA-ICP-MS); it is a quartzite from the Chiguinda Unit, part of

the presumed allochthonous Loja terrane of Litherland et al. (1994). This unit consists of quartzites and black phyllites of poorly constrained age thought to be post-Silurian based on undiagnostic miospore data (Litherland et al., 1994).

<sup>1</sup>GSA Data Repository item 2007110, Tables DR1, DR2, DR3, and DR4, is available on the Web at <http://www.geosociety.org/pubs/ft2007.htm>. Requests may also be sent to [editing@geosociety.org](mailto:editing@geosociety.org).



**Figure 4.** Field photographs from the northern part of the Eastern Cordillera of Peru. (A) Sheared granodioritic gneisses of the Sitabamba orthogneiss. Sample DC 05/6–5, which yields a U-Pb secondary ion mass spectrometry (SIMS) zircon intrusion age of  $445.9 \pm 2.4$  Ma, was collected at this locality. Lens cap is 6 cm across. (B) Foliated leucosomes within high-grade metasediments of the Marañon Complex. Sample DC 05/5–7, which yields a U-Pb SIMS zircon age of  $477.9 \pm 4.3$  Ma for leucosome development, was collected at this locality. The Marañon Complex host rock was also sampled for detrital zircon analyses (DC 05/5–4) in a zone that did not exhibit leucosome development. Pencil is 15 cm long. (C) Hualluniyoc adamellite, demonstrating the foliated nature of the intrusion, basic enclaves, and late-stage brittle deformation. Sample SU 03–20, which yields a U-Pb thermal ionization mass spectrometry (TIMS) zircon intrusion age of  $325.43 \pm 0.57$  Ma, was collected at this locality. Lens cap is 6 cm across.



Sample 99RS65 (Fig. 2) is a phyllite selected for detrital zircon LA-ICP-MS dating from the Isimanchi Formation, which forms part of the Amazonian cratonic cover. It consists of very low-grade phyllites and marbles and has a poorly constrained Carboniferous–Late Triassic age based on fish remains (Litherland et al., 1994).

### Northern Peru

Sample AM076 (Figs. 2 and 3A) is a strongly foliated greenschist-facies Marañon Complex psammite selected for detrital zircon LA-ICP-MS U-Pb dating from the type area of the Marañon Complex—the Marañon valley north of Pataz in northern Peru. Here the Marañon Complex is locally overlain by Middle Ordovician graptolite-bearing slates of the Contaya Formation (Wilson and Reyes, 1964), but opinion is divided on whether this contact is conformable or an orogenic unconformity (Haerberlin, 2002).

Samples DC 04/5–2 and DC 05/6–5 (Figs. 2 and 3A) are strongly foliated granodiorites (defined here as the Sitabamba orthogneiss) with conspicuous augen of relic igneous plagioclase and development of metamorphic biotite and garnet (Fig. 4A). The Sitabamba orthogneiss intrudes the Marañon Complex in the southwest

portion of the Marañon Complex outcrop (Fig. 3A; Wilson et al., 1995). Thermobarometric estimates for the metamorphic assemblages are  $700^\circ\text{C}$  and 12 kbar (Chew et al., 2005). Sample DC 04/5–2 was selected for precise U-Pb zircon dating using isotope-dilution thermal ionization mass spectrometry (TIMS) techniques, to constrain the timing of intrusion and LA-ICP-MS dating of inherited zircon cores. Sample DC 05/6–5 was selected for U-Pb ion-microprobe dating to constrain the timing of intrusion further to the southeast (Fig. 3A).

Samples DC 05/5–4 and DC 05/5–7 (Figs. 2 and 3A) were also taken from the Marañon Complex. The metamorphic grade of the Marañon Complex in this region is substantially higher than in that to the south (e.g., sample AM076), and consists of biotite-garnet paragneisses intruded by a series of leucosomes that share the same foliation as the country rock (Fig. 4B). DC 05/5–4 is a sample of the high-grade paragneiss host rock that was selected for detrital zircon LA-ICP-MS U-Pb dating. Particular care was taken during sampling and subsequent sample preparation to ensure that no visible leucosome vein material was present. DC 05/5–7 was sampled from a thick, foliated leucosome (5 m across) for

U-Pb ion-microprobe dating to constrain the timing of leucosome development.

Sample DC 05/5–10 (Fig. 3A) is from a 10-cm-thick fine-grained granodioritic dike that cuts the regional gneissic fabric in the Marañon Complex and is presumably related to the nearby Balsas granodiorite pluton of presumed Mississippian age (Fig. 3A). The Balsas pluton has yielded a K-Ar biotite age of  $347 \pm 7$  Ma (Sanchez, 1983). This post-tectonic dike was selected for U-Pb ion-microprobe dating to provide a minimum age on the timing of deformation in the region.

### Central Peru

Sample SU 03–19 (Figs. 3B and 3C) was taken from the Pacococha adamellite, which cuts the Marañon Complex in central Peru. It is post-tectonic with respect to the ductile deformation fabrics in the Marañon Complex and is overlain unconformably by Mississippian sediments (Fig. 3C; Mégar, 1978). It is undeformed on a hand specimen scale, but magmatic biotite is pervasively chloritized, and the pluton is prominently jointed with a series of vertical basic dikes exploiting the fissures (Fig. 3C; Mégar, 1978). The sole existing age constraint is a K-Ar biotite age of  $346 \pm 10$  Ma (Mégar,

1978). This sample was selected for U-Pb ion-microprobe dating to provide a minimum age for the timing of deformation in the region.

Sample SU 03–20 (Figs. 3B and 3D) was selected from the Hualluniyoc adamellite, one of the intrusions sampled for this study in the area of Tarma. It is strongly foliated in the field and contains abundant basic enclaves (Fig. 4C). It contains abundant minor faults, and primary igneous biotite is altered to chlorite. The pervasive brittle deformation affecting both the Pacococha and Hualluniyoc adamellites is schematically illustrated in the cross sections of Figures 3C and 3D. The pluton is locally overlain by Late Permian sediments and cuts volcanoclastic sediments of Mississippian age and was thus regarded as a late Hercynian intrusive by Mégard (1978). This sample was selected for U-Pb TIMS zircon dating.

Sample SU 03–21 (Figs. 3B and 3D) was sampled from the Huacapistana Granite of Mégard (1978) west of Tarma, which is a foliated migmatitic granite that occurs within the main belt of Marañon Complex outcrop (Fig. 3D). It is regarded as having formed coeval with the second phase of deformation in the Marañon Complex and thus is Precambrian in age (Mégard, 1978). It was sampled for U-Pb ion-microprobe dating to provide a constraint on the timing of deformation in the region.

Sample SU 03–22 (Figs. 3B and 3D) was taken from the Utcuyacu Granite west of Tarma. This is a nondeformed monzonitic granite that cuts all fabrics in the Marañon Complex and is regarded as Andean (Cretaceous to Neogene) in age (Mégard, 1978). This sample was selected for U-Pb TIMS zircon dating to constrain the timing of deformation in the Marañon Complex.

Samples SU 03–24 and SU 03–25 (Figs. 2, 3b, and 3D) were also sampled from the Marañon Complex. Sample SU 03–24 is a foliated migmatitic paragneiss that closely resembles the migmatitic Huacapistana Granite. Sample SU 03–25 is foliated garnet-biotite schist from the Marañon Complex. Thermobarometric estimates for the metamorphic assemblage are 600 °C and 11 kbar (Chew et al., 2005). Sample SU 03–24 was selected for U-Pb ion-microprobe zircon dating to constrain the timing of intrusion and LA-ICP-MS dating of inherited zircon cores. Sample SU 03–25 was selected for detrital zircon dating by LA-ICP-MS.

## U-Pb GEOCHRONOLOGICAL DATA

### ICP-MS Dating of Detrital and Inherited Zircon

U-Pb dating of detrital zircons from clastic sediments is a powerful tool for determining sedimentary provenance and crustal evolution. Additionally, the spatial resolution afforded by in situ techniques (e.g., ion microprobe or LA-ICP-MS) has enabled analysis of zircon crystals that exhibit multiple stages of growth. When combined with detailed cathodoluminescence (CL) imaging, source information can therefore also be obtained from inherited detrital zircons in granitic magmas derived from melting of sedimentary rocks at depth (e.g., Zeck et al., 2004). In situ LA-ICP-MS U-Pb zircon ages were obtained from samples AM076, 99RS28, 99RS65, DC 05/5–4, and SU 03–25 (clastic metasediments) and samples DC 04/5–2 and SU 03–24 (S-type granitic melts with abundant, large inherited zircon cores). U-Pb isotopic data and calculated U-Pb ages are listed in Table DR1. Tables DR1–DR4 are in the GSA Data Repository (see footnote 1), while detailed analytical techniques are described in the Appendix. Combined U-Pb age probability-density-distribution (PDD) plots and histograms (which illustrate concordant data only, i.e., where the error ellipse intersects the concordia) are shown as insets A to F in Figure 2 and are discussed later.

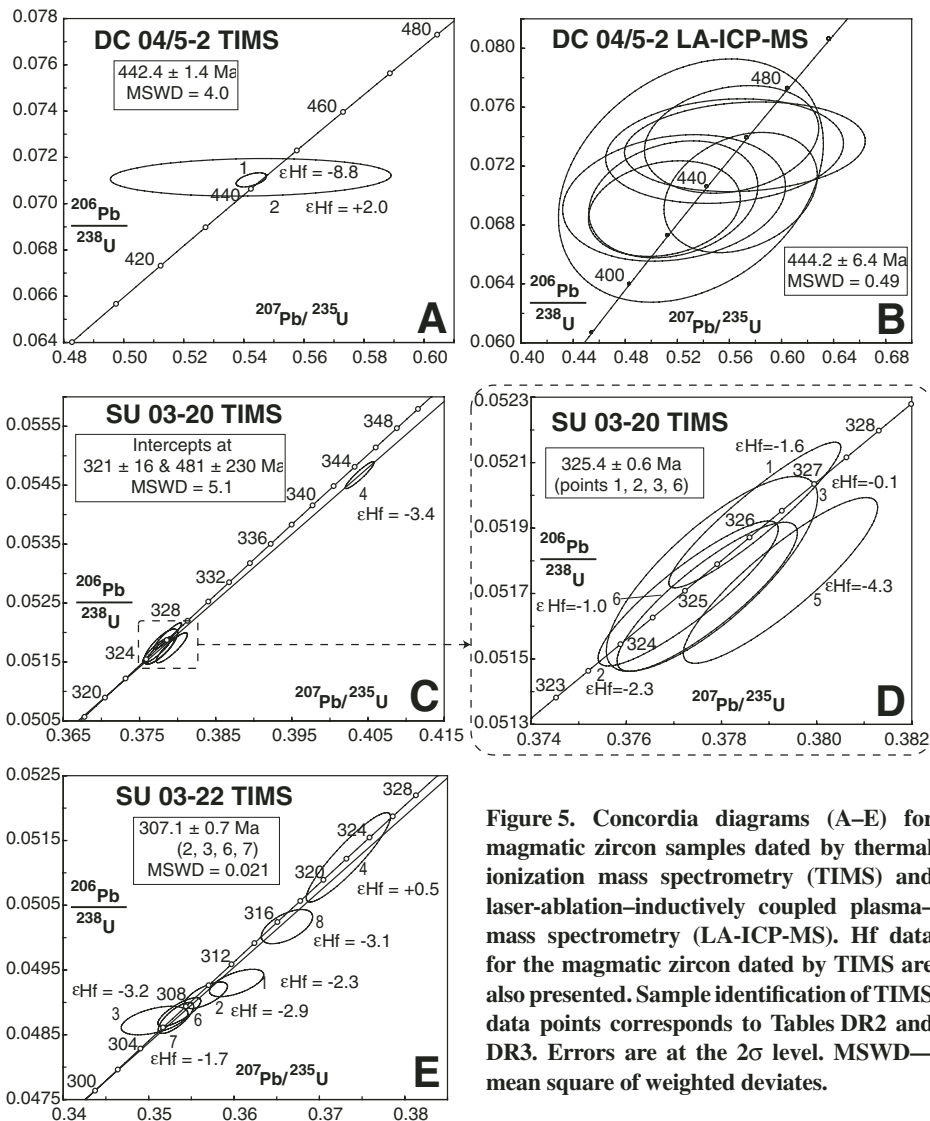


**Figure 5.** Concordia diagrams (A–E) for magmatic zircon samples dated by thermal ionization mass spectrometry (TIMS) and laser-ablation–inductively coupled plasma–mass spectrometry (LA-ICP-MS). Hf data for the magmatic zircon dated by TIMS are also presented. Sample identification of TIMS data points corresponds to Tables DR2 and DR3. Errors are at the  $2\sigma$  level. MSWD—mean square of weighted deviates.

### U-Pb TIMS and LA-ICP-MS Dating and Initial Hf Isotopic Composition of Magmatic Zircon

U-Pb isotopic data, calculated U-Pb ages, and zircon morphologies are listed in Table DR2, and Hf isotopic compositions of the dated zircon are listed in Table DR3 (see footnote 1). U-Pb concordia diagrams are illustrated in Figure 5, and detailed analytical techniques are described in the Appendix.

The crystallization of the granodioritic protolith of the Sitabamba orthogneiss in northern Peru (DC 04/5–2; Figs. 2 and 3A) has been constrained by both U–Pb TIMS dating of a distinct subpopulation of acicular magmatic zircon (two concordant single-grain analyses yielding a concordia age of  $442.4 \pm 1.4$  Ma; Fig. 5A) and LA-ICP-MS U–Pb dating of coarse (up to 50  $\mu\text{m}$  thick) rims of magmatic zircon (concordia age [Ludwig, 1998] of  $444.2 \pm 6.4$  Ma; Fig. 5B). Further TIMS data only yielded strongly discordant points and are not shown. There was only a limited amount of Hf isotopic data for this sample (as there were only two TIMS data points), but the difference in  $\epsilon_{\text{Hf}(T)}$  values of  $-8.8$  and  $+2.0$  for the two dated zircon grains was substantially larger than the range shown by other samples (Table DR3 [see footnote 1]; Fig. 5A).

The Huallunuyoc adamellite (SU 03–20; Figs. 3B and 3D) yielded a concordia age of  $325.4 \pm 0.6$  Ma based on four concordant data points (Figs. 5C and 5D). Dated zircons were slightly pinkish,  $\sim 200$   $\mu\text{m}$  long, and were prismatic to long prismatic (length:width ratio [l:w] = 4:1); their morphology corresponded to type S22 on a Pupin typogram (Pupin, 1980). Some crystals contained elongate and rounded melt inclusions. One zircon (Fig. 5C) yielded a discordant analysis that pointed to an inherited component of a  $481 \pm 230$  Ma age. Although this upper intercept age was poorly constrained, it should be noted the ca. 480 Ma peak was very prominent in the LA-ICP-MS detrital zircon data. The  $\epsilon_{\text{Hf}(T)}$  values of the four concordant data points ranged from  $-2.3$  to  $-0.1$  (Table DR3 [see footnote 1]; Fig. 5D). The two discordant analyses 4 and 5 had lower  $\epsilon_{\text{Hf}(T)}$  values of  $-3.4$  and  $-4.3$ , consistent with an older crustal source for the Hf.

The Utcuyacu Granite (SU 03–22; Figs. 3B and 3D) yielded a concordia age of  $307.1 \pm 0.7$  Ma based on four concordant data points (analyses 2, 3, 6, 7; Fig. 5E). Dated zircons were  $\sim 80$   $\mu\text{m}$  long and were short prismatic. They also corresponded to a type S22 morphology on a Pupin typogram (Pupin, 1980). Most crystals contained abundant inclusions, some of which were found in the center of the crystal and which probably represented cores. Two separate zircons yielded older concordia ages of 316 Ma and 322 Ma (Fig. 5E). These zircons were presumably xenocrysts derived locally from the Carboniferous magmatic arc that had been incorporated into the melt. The  $\epsilon_{\text{Hf}(T)}$  values of all the data points ranged from  $-3.2$  to  $+0.5$  (Table DR3 [see footnote 1]; Fig. 5A).

#### U–Pb Ion-Microprobe Dating of Zircon

U–Pb isotopic data and calculated U–Pb ages are listed in Table DR4 (see footnote 1).

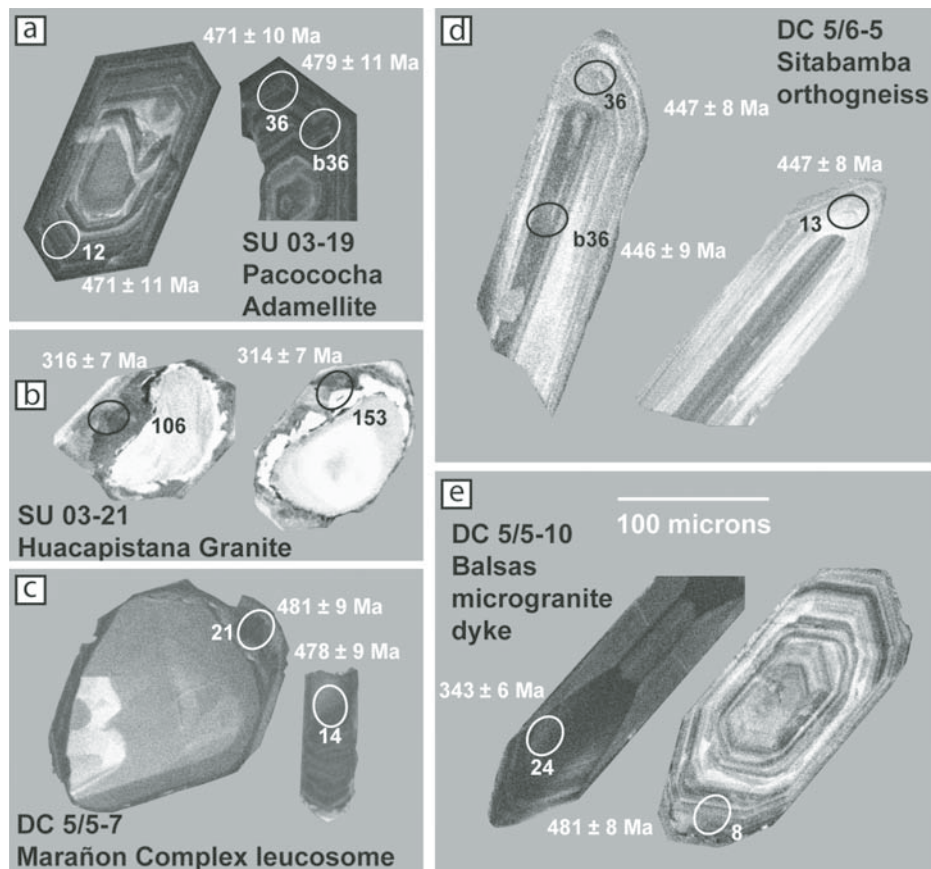


**Figure 6. Representative zircon petrography for secondary ion mass spectrometry (SIMS) analyses: scanning electron microscope–cathodoluminescence images from (A) Pacococha adamellite, (B) Huacapistana Granite, (C) leucosome within the Marañon Complex, (D) Sitabamba orthogneiss, and (E) Carboniferous microgranite dike. Sample identification of SIMS data points corresponds to Table DR4 (see text footnote 1). All quoted ages are concordia ages, and uncertainties are at the  $2\sigma$  level. All images use the scale bar in E.**

Scanning-electron micrograph (SEM) CL images of representative dated zircons are illustrated in Figure 6, and U–Pb Tera–Wasserburg concordia diagrams are illustrated in Figure 7. A common Pb correction was only applied to samples that exhibited significant levels of  $^{204}\text{Pb}$ . Detailed analytical techniques are described in the Appendix.

#### Central Peru

The Pacococha adamellite (SU 03–19; Figs. 3B and 3C) yielded a single zircon population consisting of short prismatic, orange-brown grains (l:w of  $\sim 2:1$ ). Grains were typically  $\sim 150$ – $200$   $\mu\text{m}$  long and were euhedral with well-developed terminations (Fig. 6A). The grains were dark under CL and exhibited oscillatory zoning. No inherited cores were analyzed, and 13 spots from the rims of nine separate crystals yielded a concordia age of  $474.2 \pm 3.4$  Ma. Th/U ratios of the magmatic rims typically clustered between 0.1 and 0.35,

and the spots were uncorrected for common Pb (Table DR4, see footnote 1).

The Huacapistana Granite (SU 03–21; Figs. 3B and 3D) and the Marañon Complex migmatitic paragneiss (SU 03–24; Figs. 2, 3B, and 3D) closely resembled each other in terms of their zircon populations. They will be considered together, and the CL images of SU 03–21 (Fig. 6B) can be considered representative of SU 03–24. The population consisted of medium-sized (between 100 and 200  $\mu\text{m}$  in diameter), colorless, well-faceted grains. The grains were typically subspherical or stubby prisms. Under CL, all grains contained inherited cores that formed the majority of the crystal. The inherited cores were nearly always rounded but exhibited a wide variety of internal zoning and CL intensity patterns. The boundary between the inherited core and the magmatic rim was commonly characterized by a thin (1–5  $\mu\text{m}$ ) black zone under CL, which was

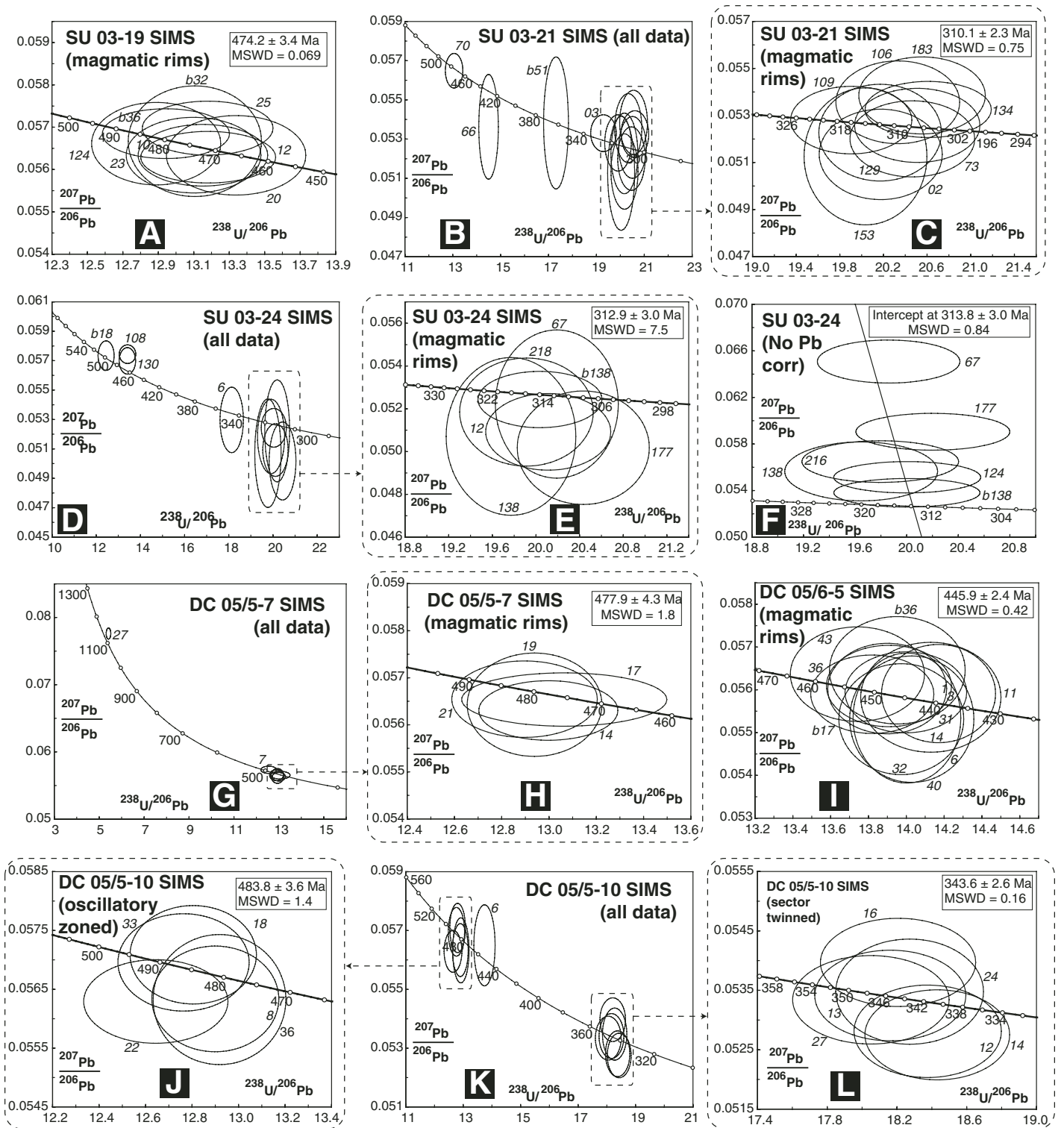


Figure 7. Tera-Wasserburg concordia diagrams (A–L) showing zircon ages for samples dated by secondary ion mass spectrometry (SIMS). Spot numbers are those given in Table DR4 (see text footnote 1). MSWD—mean square of weighted deviates.

sometimes overgrown by a bright white zone of irregular thickness. The succeeding outer portions of the crystal typically displayed an irregular zoning pattern and were gray under CL (Fig. 6). The total thickness of the rim was seldom greater than 40  $\mu\text{m}$ . Where possible, analyses were confined to the gray outer portions of the rim. Inherited cores for both samples yielded ages that ranged between 500 and 340 Ma (Figs. 7B and 7D). Eight spots from the rims on eight separate grains yielded a concordia age of  $310.1 \pm 2.3$  Ma (Fig. 7C) for sample SU 03–21. Six spots from the rims of six separate grains yielded a concordia age of  $312.9 \pm 3$  Ma (Fig. 7E) for sample SU 03–24, albeit with a relatively high mean square of weighted deviates (MSWD) of 7.5. Th/U ratios from the rims of both samples were typically extremely low, clustering around 0.01 (Table DR4, see footnote 1). Three out of eight rims in sample SU 03–21 were corrected for common Pb, while all six rims in sample SU 03–24 were corrected for common Pb (Table DR4, see footnote 1). Five of these six analyses are shown uncorrected for common Pb on an inverse concordia diagram (Fig. 7F). They yield an intercept age of  $313.8 \pm 3.0$  Ma (MSWD = 0.84), assuming the anchor for the intercept has a present-day average terrestrial common Pb composition of  $^{207}\text{Pb}/^{206}\text{Pb} = 0.83$  (Stacey and Kramers, 1975), which corroborates the accuracy of the common Pb correction.

#### Northern Peru

The Mara $\tilde{\text{a}}$ on Complex leucosome (DC 05/5–7; Figs. 2 and 3A) yielded an extremely diverse population of zircons. The majority of the population was composed of large (often up to 200  $\mu\text{m}$  in diameter) faceted grains (which were either long prismatic, short prismatic, or subspherical in habit, with a discrete subpopulation of small prismatic, euhedral zircons that rarely exceeded 100  $\mu\text{m}$  in length). Under CL, the distinction between the two subpopulations was clear. The small euhedral prisms were CL dark and had faint idiomorphic zoning (Fig. 6C) with rare inherited cores. The coarser grains showed a thin (10–30  $\mu\text{m}$ ) CL dark rim with faint idiomorphic zoning, which surrounded a large inherited core that made up the majority of the zircon crystal (Fig. 6C). The inherited cores exhibited a wide variety of forms, zoning patterns, and CL intensities, which reflect the variable nature of the precursor detrital zircon population. Four spots from the CL dark regions on four separate grains yielded a concordia age of  $477.9 \pm 4.3$  Ma (Fig. 7H), which is interpreted as the crystallization age of the leucosome. Both the large faceted grains and the small prismatic grains were analyzed (Fig. 6C). One inherited

core (27) was analyzed and yielded a  $^{206}\text{Pb}/^{238}\text{U}$  age of  $1093 \pm 16$  Ma, while another analysis (7), which yielded an age marginally older than the concordia age ( $^{206}\text{Pb}/^{238}\text{U}$  age of  $494 \pm 10$  Ma), is interpreted as a mixture between a magmatic rim and inherited core. Th/U ratios of the magmatic rims were typically extremely low, averaging around 0.05 (Table DR4, see footnote 1). All four magmatic spots were corrected for common Pb (Table DR4, see footnote 1).

The Sitabamba orthogneiss (DC 05/6–5; Figs. 2 and 3A) yielded one population of long prismatic (up to 300  $\mu\text{m}$  long) zircons that were predominantly euhedral with sharp terminations (Fig. 6D). CL images exhibited bright oscillatory zoned rims that commonly surrounded a slightly darker oscillatory zoned core. The percentage of the population that contained potentially inherited cores is estimated at less than 5%, although no such grains were analyzed. Eleven spots from the CL bright marginal regions on nine separate grains yielded a concordia age of  $445.9 \pm 2.4$  Ma (Fig. 7J), which is interpreted to be the age of intrusion. Th/U ratios of the dated zircons clustered between 0.1 and 0.4, although one outlier (13) had a Th/U ratio >1 (Table DR4, see footnote 1). Analyses were uncorrected for common Pb (Table DR4, see footnote 1).

The Balsas microgranite dike (DC 05/5–10; Fig. 3A) yielded two major populations of zircons. The first population consisted of elongate prismatic zircons (typically between 200 and 250  $\mu\text{m}$  long) that were euhedral with sharp terminations (Fig. 5E). They were CL dark and displayed a characteristic sector zoning. The second population consisted of stubby prismatic zircons (l:w typically of ~2:1) that were also euhedral with well-developed terminations. CL images exhibited a prominent oscillatory zoning. Neither population exhibited clear inherited cores. These two morphologies comprised ~95% of the total zircon population. Six spots from six separate grains from the sector-zoned population yielded a concordia age of  $343.6 \pm 2.6$  Ma (Fig. 7L), which is interpreted to be the intrusion age of the dike. These analyses were characterized by Th/U ratios between 0.35 and 0.5 (Table DR4, see footnote 1). Five spots from five separate grains from the oscillatory zoned population yielded a concordia age of  $483.8 \pm 3.6$  Ma (Fig. 7J). These analyses were typically characterized by Th/U ratios less than 0.1 (Table DR4, see footnote 1). One grain that did not conform to the two zircon morphologies described above was also analyzed. It yielded a  $^{206}\text{Pb}/^{238}\text{U}$  age of  $453 \pm 10$  Ma (Fig. 7K, spot 6) and was characterized by a high Th/U ratio of >0.9 (Table DR4, see footnote 1). The spots were uncorrected for common Pb (Table DR4, see footnote 1).

## TECTONIC EVOLUTION OF THE EASTERN CORDILLERA OF PERU

### Central Peru

U-Pb zircon data from the sampling transect in the Eastern Cordillera of Central Peru clearly demonstrate that the Mara $\tilde{\text{a}}$ on Complex has been affected by two major orogenic events. The post-tectonic Pacococha adamellite (SU 03–19; Figs. 3B and 3C) constrains all polyphase deformation within the Mara $\tilde{\text{a}}$ on Complex prior to  $474.2 \pm 3.4$  Ma (Fig. 7A). However, 25 km to the southeast, the syn-D2 migmatitic Huacapistana granite (SU 03–21; Figs. 3B and 3D) and syn-D2 migmatitic paragneisses in the Mara $\tilde{\text{a}}$ on Complex (SU 03–24; Figs. 2, 3B, and 3D) yielded ages of  $310.1 \pm 2.3$  Ma and  $312.9 \pm 3.0$  Ma, respectively (Figs. 7C and 7E). The timing of this Pennsylvanian (ca. 312 Ma) tectonothermal event is corroborated by the presence of deformed plutons at  $325.43 \pm 0.57$  Ma (Hualluniyoc adamellite, SU 03–20; Figs. 3B, 3D, and 5D) and entirely undeformed plutons at  $307.05 \pm 0.65$  Ma (Utcuyacu granite, SU 03–22; Figs. 3B, 3D, and 5E).

Detrital zircon data have been obtained from a Mara $\tilde{\text{a}}$ on Complex meta-sandstone (SU 03–25) from the same transect (Figs. 3B and 3D) that had been affected by the late Carboniferous (ca. 312 Ma) tectonothermal event. Although the age spectrum is not illustrated on Figure 2 due to the small number of analyses ( $n = 15$ ), the presence of young grains at ca. 470 Ma (Table DR1, see footnote 1) implies that this sample has undergone post-470 Ma metamorphism. The data from the Mara $\tilde{\text{a}}$ on Complex in central Peru suggest that it is composed of two separate units: an older unit that underwent metamorphism prior to 474 Ma, and a younger unit (which contains detritus presumably derived from the ca. 470 Ma magmatic belt) that was deformed ca. 312 Ma. The contact between these two units remains uncertain, but it should be noted that the region was strongly deformed during the main compressional phase of the Andean orogeny (the late Eocene Incaic phase; Steinmann, 1929) and that the precise locations of many of the Andean thrusts remain speculative, particularly where they affect the lithologically monotonous metasediments of the Mara $\tilde{\text{a}}$ on Complex.

### Northern Peru

U-Pb zircon data from the sampling transect in the Eastern Cordillera of northern Peru also demonstrate that the Mara $\tilde{\text{a}}$ on Complex has been affected by at least two major orogenic events. A foliated leucosome from garnet-bearing

paragneisses in the Marañon Complex yielded a concordia age of  $477.9 \pm 4.3$  Ma (DC 05/5–7; Figs. 2, 3A, and 7H), which is interpreted as dating leucosome generation. It is suggested that this event correlates with the pre–474 Ma deformation in central Peru, i.e., there was a ca. 478 Ma orogenic event that affected part of the Marañon Complex for several hundred kilometers along the Eastern Cordillera. Importantly, the paragneiss host rock (DC 5–5–4) to the leucosomes contained no zircons younger than ca. 750 Ma (Fig. 2C; Table DR1 [see footnote 1]).

The presence of a younger orogenic event in northern Peru is indicated by two separate lines of evidence. First, the protolith to the Sitabamba orthogneiss (samples DC 04/5–2 and DC 05/6/–5; Figs. 2 and 3A) crystallized between 442 and 446 Ma (Figs. 5A, 5B, and 7J), and, therefore, the high-grade metamorphic assemblages (700 °C, 12 kbar; Chew et al., 2005) in the orthogneiss must postdate this. Second, a strongly deformed greenschist-facies Marañon Complex psammite (AM076; Figs. 2D and 3A) contains a prominent peak in the detrital zircon population at ca. 470 Ma (Fig. 2D; Table DR1 [see footnote 1]) not seen in the older Marañon Complex rocks. For the purposes of discussion here, these two units are termed the “Old” and “Young” Marañon Complexes, respectively (e.g., Fig. 8D). The young Marañon Complex rocks must have undergone post–470 Ma orogenesis, and we tentatively correlate this event with the post–442 Ma event experienced by the Sitabamba orthogneiss. However, this event is older than the Pennsylvanian (ca. 312 Ma) event seen in central Peru because the young Marañon Complex rocks in northern Peru (with the prominent ca. 470 Ma detrital zircon peak) are unconformably overlain by Mississippian (ca. 340 Ma) sediments (Wilson and Reyes, 1964).

### Interpretation and Correlation with Events in the Arequipa-Antofalla Basement

With the present data, we can reliably constrain two orogenic events in the Eastern Cordillera of Peru at ca. 478 Ma and ca. 312 Ma, and loosely constrain a third to 440–340 Ma. The ca. 478 Ma event is interpreted to be of regional extent, and the Neoproterozoic age previously assigned to this metamorphism (Dalmayrac et al., 1980) is interpreted to be a result of unresolved multiple inheritance in bulk, unabraded zircon fractions.

These data also demonstrate the existence of an Ordovician-Silurian magmatic belt (474–442 Ma) in the Eastern Cordillera of Peru. These plutons (the Sitabamba orthogneiss and the Pacococha adamellite) have chemistry compatible with formation at a continental

subduction zone (high large ion lithophile element [LILE]/high field strength element [HFSE] ratios, negative Nb anomalies) similar to the Ordovician-Silurian magmatic rocks that intrude the Proterozoic gneisses of the Arequipa-Antofalla basement (Loewy et al., 2004; Mukasa and Henry, 1990). Recent geochronological studies employing U-Pb TIMS single zircon dating have demonstrated that the majority of early Paleozoic arc-related magmatism in the Arequipa-Antofalla Block falls within the 476–440 Ma age range (Loewy et al., 2004), very similar to the age range for magmatism in the Eastern Cordillera quoted here. Additionally, there is evidence for Ordovician metamorphism in the Arequipa-Antofalla basement (Loewy et al., 2004). Greenschist-facies metamorphism in southern Peru occurred after the intrusion of a  $464 \pm 4$  Ma megacrystic granite at Ocona and prior to the emplacement of undeformed granites at Mollendo at  $468 \pm 4$  Ma (Loewy et al., 2004), and amphibolite-facies metamorphism occurred at Belén in northern Chile prior to the intrusion of massive granodiorites at  $473 \pm 2$  Ma and  $473 \pm 3$  Ma (Loewy et al., 2004).

Combined, these data demonstrate the presence of an Early Ordovician magmatic and metamorphic belt that runs along the western margin of the Arequipa-Antofalla basement and is offset northeastward into the Eastern Cordillera (Fig. 8). We suggest that the change in strike of the belt results from the presence of an original embayment on the western Gondwanan margin during the early Paleozoic. This embayment was then filled by subsequent accretion of oceanic material (which represents the basement to the Western Cordillera; Polliand et al., 2005), probably during the Carboniferous (Mišković et al., 2005).

### INTERPRETATION OF THE DETRITAL ZIRCON DATA

In interpreting these data, the relationship of the sedimentary sequences (or the crustal blocks from which the granitic melts inherited their zircon) with respect to the Gondwanan margin is critical. If the units are autochthonous (or paraautochthonous), then the detrital zircon age signatures obtained can be used to constrain the paleogeography of the hinterland—the Gondwanan margin of the north-central Andes. The detrital zircon spectrum itself cannot be used to assess the exotic status of the units in question. Currently, there is a very limited data set for the early Paleozoic sequences within the Andean belt, so the characteristic detrital zircon signature of this margin (if one indeed exists) is not known. Detrital zircon data do exist for Early Cambrian sandstones from the Argentine

Precordillera (Thomas et al., 2004), but this terrane is exotic to the Gondwanan margin (Dalla Salda et al., 1992). In considering the detrital zircon data presented here, we consider the Isimanchi Formation of the Cordillera Real of Ecuador (99RS65) to be autochthonous with respect to the Gondwanan margin, since it is a cratonic cover sequence (Litherland et al., 1994), and thus its detrital zircon spectrum can be used to reconstruct the evolution of this segment of the Gondwanan margin. Additionally, the Marañon Complex is commonly accepted as an autochthonous Gondwanan margin sequence (e.g., Haeberlin, 2002). The status of the other units and crustal blocks is uncertain. The Chiguinda Unit of the Cordillera Real was thought to be allochthonous (Litherland et al., 1994), but recent research suggests an autochthonous origin (Pratt et al., 2005). The similar detrital age distributions in the two samples would be consistent with an autochthonous origin for the Chiguinda Unit. Clearly, it is difficult to assess whether the crustal blocks that were the source of the sampled granitic melts are autochthonous or allochthonous, but the country rock at the depth of emplacement is composed of presumed autochthonous Marañon Complex metasediments.

The majority of samples exhibit a prominent peak between 0.45 and 0.5 Ga, which temporally overlaps with the onset of subduction-related magmatism in the Eastern Cordillera of Peru (this study), the Famatinian arc (Fig. 1) of northern Argentina (Lork and Bahlburg, 1993; Pankhurst et al., 1998), Patagonia (Pankhurst et al., 2006), the Arequipa-Antofalla basement of southern Peru and northern Chile (Fig. 1; Loewy et al. 2004), Venezuela (the Caparo Arc of Bellizzia and Pimentel, 1994), and Colombia (Boinet et al., 1985). Further prominent peaks are found within the ca. 0.5–0.65 Ga age range, and these ages are typical of the Brasília–Pan African orogenic cycles. Significantly, less detritus lies within the ca. 0.7–0.9 Ga age range (this trend is particularly evident in samples DC 04/5–2 and SU 03–24). Between a third and a half of all grains in each sample lie within the 0.9–1.3 Ga age range, and the largest peaks are commonly encountered between 1 and 1.2 Ga. These ages are comparable to the Elzevirian orogeny of the Grenville orogen, or the Sunsas orogen of the southwest Amazonian craton (Fig. 1; Santos et al., 2002). With the exception of sample DC 04/5–2, there is a very limited amount of detritus in the 1.3–1.7 Ga age range. Very minor peaks are encountered at 1.7–1.9 Ga and at ca. 2.6 Ga in some samples, but the amount of detritus older than ca. 2 Ga is minimal. The tectonic significance of the detrital zircon data is discussed next and combined with the U-Pb zircon magmatic and metamorphic

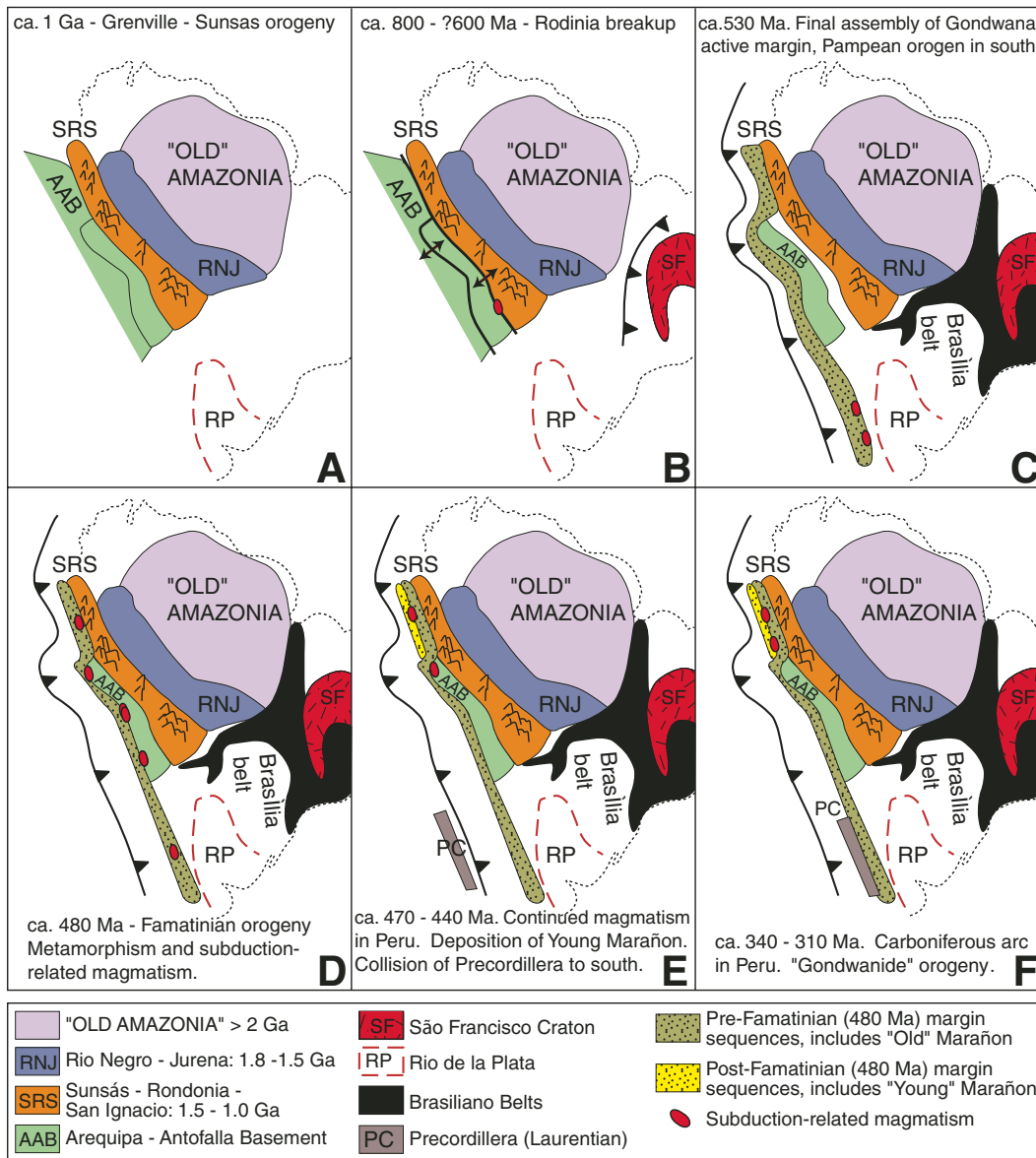


Figure 8. Schematic reconstruction of the evolution of the Gondwanan margin of the north-central Andes. Basement geology is from Cordani et al. (2000), sequence of tectonic events on the south-central proto-Andean margin is from the summary of Ramos and Aleman (2000), and sequence of tectonic events on the north-central proto-Andean margin is from this study.

constraints described previously to produce a model for the evolution of the proto-Andean margin of the north-central Andes.

### EVOLUTION OF THE GONDWANAN MARGIN OF THE NORTH-CENTRAL ANDES

#### Pre-Gondwanan history (1000–600 Ma)

Figure 8 is a schematic reconstruction of the evolution of the Gondwanan margin of the north-central Andes. The Sunsas orogen of the southwest Amazonian craton is invoked as a potential source region for the abundant ca. 0.9–1.3 Ga peaks observed in the detrital zircon populations. We infer that the Sunsas orogen continues

in a northwestern direction underneath the thick pile of foreland sediments to the east of the northern Andes (Fig. 1), where it is likely to be contiguous with the ca. 1 Ga gneissic basement inliers in the Colombian Andes (Fig. 8A; Restrepo-Pace et al., 1997; Cordani et al., 2005). The Arequipa-Antofalla basement is likely to have accreted at this time (Loewy et al., 2004). Since the amount of older detritus is minimal, the Sunsas orogen might have served as a “topographic barrier” to the transport of detritus from the Paleoproterozoic–Archean core of the Amazonian craton (Fig. 8A).

The time period between 800 and 600 Ma (Fig. 8B) is represented by a very small amount of detritus in the detrital zircon spectra (Fig. 2), but the source is uncertain. During this time,

Laurentia detached from the Rodinian supercontinent, contemporaneous with the amalgamation of the East and West Gondwana cratons (Hoffman, 1991; Dalziel, 1991; Figures 11 and 12 in Dalziel 1997; Meert and Torsvik, 2003; Pisarevsky et al., 2003). There is little evidence on the western Gondwanan margin for magmatism at this time, although this is at least partly due to the restricted amount of Precambrian basement exposed within the Andean belt. Juvenile extensional magmatism (dacite dikes) has been dated at  $635 \pm 4$  Ma in the Arequipa-Antofalla basement of northern Chile (Loewy et al., 2004). This rifting event probably involved the partial detachment of the Arequipa-Antofalla basement, which was subsequently reaccreted during the Pampean orogen (Loewy et al., 2004).

A-type orthogneisses of mid-Neoproterozoic age ( $774 \pm 6$  Ma) have been documented from the Grenvillian basement of the Precordillera terrane and are interpreted as representing the breakup of Rodinia (Baldo *et al.*, 2006). Extension-related volcanism related to the breakup of Rodinia has been identified in the Puncoviscana fold belt of northwestern Argentina (Omarini *et al.*, 1999), but this volcanism is primarily basic in nature and is therefore unlikely to be a significant source of zircon.

Other potential sources include the Precambrian (ca. 650–580 Ma) basement of eastern Venezuela (Marechal, 1983) or the north-south-trending Brasília belt, which developed in response to the convergence of the Amazonian and São Francisco cratons (Fig. 1). The Brasília belt contains both 0.8–0.7 Ga syncollisional granitoids and 0.9–0.63 Ga arc meta-tonalites and meta-granodiorites (Pimentel *et al.*, 1999). However, the southwestward extensions of the Brasília belt toward the western Gondwanan margin (the Paraguay belt and the Tucavaca belt of Bolivia) are younger (0.6–0.5 Ga; Pimentel *et al.*, 1999) and thus cannot have been a source of detritus for the time period in question. It is difficult to envisage how the Brasília belt could have been a source for the early Paleozoic basins of the western Gondwanan margin when there is minimal detritus from the intervening Amazonian craton.

### The Active Gondwanan Margin

By the onset of the Phanerozoic (Fig. 8C), the entire western part of the Gondwana margin was active. This was the inception of the Terra Australis orogen (Cawood, 2005; see Fig. 3). A synthesis of the Paleozoic accretionary history of the proto-Andean margin of Gondwana is given by Ramos and Aleman (2000).

Figure 8C illustrates the margin sequences of the north-central Andes, which would include the old Marañon Complex identified in this study and the Chiquerío and San Juan Formations, which rest unconformably on the Arequipa-Antofalla basement in southern Peru (Caldas, 1978). No magmatism has been identified in the north-central Andes at the onset of Phanerozoic (Fig. 8C) to account for the ca. 550 Ma peaks seen in some of the detrital zircon spectra (e.g., samples 99RS28, AM076), but there is abundant subduction-related granitoid magmatism and high-grade metamorphism, which initiated at ca. 530 Ma in the Sierra Pampeanas (Fig. 1) in northern Argentina (Rapela *et al.*, 1998; Lucassen and Becchio, 2003). We tentatively suggest that our detrital zircon data document the existence of an early (pre-orogenic) phase of Pampean subduction-related magmatism in

the north-central Andes that is presently buried underneath the present-day Andean chain or adjacent foreland sediments.

The new ages for major phase of metamorphism in the Eastern Cordillera of Peru, presented here as Famatinian (ca. 480 Ma) and not Neoproterozoic, as previously thought (Dalmayrac *et al.*, 1980), demonstrate that this Early–Middle Ordovician orogenic cycle runs the length of the western Gondwanan margin (Fig. 8D) and is broadly contemporaneous with the onset of Famatinian metamorphism to the south (18–34°S) (470–440 Ma; Lucassen and Franz, 2005, and references therein) and in Colombia and Venezuela (Bellizzia and Pimentel, 1994). Additionally, the existence of a subduction-related magmatic belt in the Eastern Cordillera of Peru is demonstrated, and U-Pb zircon dating of arc plutons constrains this event to 474–442 Ma. It is also represented by an important Early Ordovician peak in the detrital zircon record. This demonstrates that Famatinian-age magmatism spans the length of the margin (Figs. 8D and 8E) from Venezuela (the ca. 495–425 Ma Caparo Arc of Bellizzia and Pimentel, 1994) and Colombia (Boinet *et al.*, 1985) to northern Argentina (ca. 490–470 Ma; Pankhurst *et al.*, 2000).

The Argentine Precordillera, a terrane derived from southern Laurentia (Dalla Salda *et al.*, 1992) that collided with Gondwana in the Middle Ordovician (Ramos *et al.*, 1986), shows that Laurentian crustal fragments were clearly interacting with Gondwana during the early Paleozoic. The nature of this interaction has proved contentious (see Thomas and Astini, 2003, for a review), and various authors favor either (1) a Laurentia–western Gondwana collision, producing a continuous Taconic–Famatinian orogenic belt (e.g., Dalla Salda *et al.*, 1992; Dalziel *et al.*, 1994), (2) a connection between the Precordillera and a distal promontory on Laurentia (the Ouachita embayment), which then collided with Gondwana (e.g., Dalziel, 1997), or (3) a Precordillera microcontinent, which detached from Laurentia during the Cambrian and drifted across the Iapetus ocean basin to collide with the proto-Andean margin of Gondwana during the Ordovician (Astini *et al.*, 1995). Although it is somewhat beyond the scope of this article to present detailed arguments for the competing hypotheses, Figure 8E depicts the Precordillera terrane as a detached Laurentian microcontinent, in keeping with recent research, which emphasizes a wide separation between Laurentia and Gondwana during the Early–Middle Ordovician (Thomas *et al.*, 2002) and evidence that the Precordillera acted as an indenter during the Middle Ordovician collision episode (Astini and Dávila, 2004). Evidence from this study that Famatinian

metamorphism and magmatism was continuous along the western Gondwanan margin shows that the early Paleozoic evolution of western Gondwana was similar to that of Laurentia (the Taconic orogenic cycle) and that they had comparable tectonic histories over several thousand kilometers along strike.

The latest stages of the evolution of the north-central proto-Andean margin involved the deposition of post-Famatinian cover sequences (the young Marañon Complex of this study; Fig. 8E). These sequences contain abundant Famatinian zircon (Fig. 2). A prominent magmatic gap then appears to follow along the margin for nearly 100 m.y. The youngest phase of pre-Carboniferous magmatism in the Eastern Cordillera of Peru is dated to 442 Ma (DC 04/5–2; Fig. 5A), while the oldest Carboniferous magmatism is the 344 Ma microgranite dike (DC 05/5–10; Fig. 7L) associated with the Balsas pluton in the northern Eastern Cordillera. An identical magmatic gap has been reported in the proto-Andean margin further to the south in northern Chile and northwestern Argentina according to Bahlburg and Hervé (1997), who invoked a passive-margin setting during this period. This period of magmatic quiescence along the margin from northern Peru (5°S) to northern Chile (30°S) is slightly complicated by the Silurian–Devonian bulk fraction U-Pb zircon ages (lower intercept ages) for arc-related magmatism in the Arequipa-Antofalla basement of southern Peru (Mukasa and Henry, 1990). However, more recent single-crystal U-Pb zircon dating from the same batholith did not yield any ages younger than 440 Ma (Loewy *et al.*, 2004), and it is very likely that the lower intercept ages of Mukasa and Henry (1990) were anomalously young due to the difficulty in deconvoluting the combined effects of Pb loss and inheritance in bulk zircon U-Pb data.

The Mississippian (Fig. 8F) was marked by the renewal of subduction-related magmatism. However, the tectonic setting of the north-central proto-Andean margin is complicated. The northern parts of the margin (e.g., Venezuela) record continental collision (the Alleghenian orogeny) between Gondwana and Laurussia (Ramos and Aleman, 2000). Farther to the south, in the Eastern Cordillera of Peru, there is a transition to an active-margin setting. A phase of I-type subduction-related granitic magmatism at ca. 342–325 Ma is followed by Pennsylvanian (ca. 312 Ma) high-grade metamorphism and crustal anatexis. This event has been related to the accretion of an outboard oceanic terrane that is now buried beneath the Western Cordillera (Miškovíc *et al.*, 2005). This event is broadly contemporaneous with the Toco tectonic event and the high-pressure metamorphism

in the Sierra Limon Verde Complex of northern Chile (Bahlburg and Hervé, 1997), which is interpreted as a deformed convergent-margin accretionary complex. Additionally, a similar phase of Mississippian I-type granitic magmatism followed by Pennsylvanian S-type granites representing crustal anatexis has been identified in Patagonia (Pankhurst et al., 2006), where collisional orogeny is related to the accretion of the Deseado terrane. Combined, this phase of Pennsylvanian tectonism can be considered to be part of the Gondwanide orogeny, a pan-Pacific orogenic event that represents the terminal phase in the Terra Australis orogen (Cawood, 2005) prior to the final assembly of Pangea.

## CONCLUSIONS

The detrital zircon data from the north-central proto-Andean margin demonstrate that the basement to the western Gondwanan margin was likely composed of a metamorphic belt of Grenvillian age, upon which an early Paleozoic magmatic belt was situated in a similar way to the Sierra Pampeanas and Famatina terranes of northern Argentina. This is based on the presence of prominent peaks between 0.45–0.65 Ma and 0.9–1.3 Ga in the detrital zircon record of Paleozoic sequences in the Eastern Cordilleras of Peru and Ecuador.

Plutons associated with this early Paleozoic subduction-related magmatic belt have been identified in the Eastern Cordillera of Peru and have been dated by U-Pb zircon TIMS and ion microprobe to 474–442 Ma. This is in close agreement with the ages of subduction-related magmatism in the Arequipa-Antofalla basement (Loewy et al., 2004). This early Paleozoic arc is clearly not linear since it jumps from a coastal location in the Arequipa-Antofalla basement to several hundred kilometers inland in the Eastern Cordillera further to the north (Fig. 2). This is interpreted as an embayment on the proto-Andean margin at the time the arc was initiated; if this is the case, the northern termination of the Arequipa-Antofalla basement in the vicinity of Lima (Fig. 2) is an Ordovician or older feature.

The arc magmatism pre- and postdates phases of regional metamorphism in the Eastern Cordillera of Peru. U-Pb zircon ion-microprobe dating of zircon overgrowths in high-grade leucosomes demonstrates the presence of a metamorphic event at ca. 478 Ma and refutes the previously assumed Neoproterozoic age for orogeny in the Peruvian Eastern Cordillera. The presence of an Early to Middle Ordovician-age magmatic and metamorphic belt in the north-central Andes demonstrates that Famatinian metamorphism and subduction-related magmatism were continuous from Patagonia (Pankhurst et al., 2006)

through northern Argentina and Chile to as far north as Colombia and Venezuela, a distance of nearly seven thousand kilometers. The presence of an extremely long Early–Middle Ordovician active margin on western Gondwana invites comparison with the Taconic–Grampian orogenic cycle of the eastern Laurentia margin (which is of similar age and strike length) and supports models that have these two active margins facing each other during the Ordovician.

U-Pb zircon ion-microprobe dating of zircon overgrowths in migmatites have been dated at ca. 312 Ma, and they represent a previously unreported high-grade Gondwanide event that affected the Peruvian segment of the proto-Andean margin. The original relationship between the Carboniferous and Ordovician metamorphic belts is uncertain because they were later affected by Andean (Eocene–Oligocene) thrusting, but, overall, the pattern of crustal growth in the north-central Andes (Fig. 8F) implies that this area was dominated by a series of progressive crustal accretion events, which resulted in a series of age domains that become younger away from an old Amazonian core.

## APPENDIX

### U-Pb Zircon Geochronology

Zircons were separated from several kilograms of sample by conventional means. The sub-300  $\mu\text{m}$  fraction was processed using a Wilfey table, and then the Wilfey heavies were passed through a Frantz magnetic separator at 1 A. The nonparamagnetic portion was then placed in a filter funnel with di-iodomethane. The resulting heavy fraction was then passed again through the Frantz magnetic separator at full current. A side slope of  $1^\circ$  was used to separate nonparamagnetic zircons for TIMS and ion-microprobe analysis to maximize concordance, while a side slope of  $10^\circ$  was used for LA-ICP-MS analyses to prevent potential fractionation of the detrital population. All zircons were handpicked in ethanol using a binocular microscope, including those for detrital zircon analysis. Zircons for TIMS analyses were air-abraded to remove marginal zones that are prone to Pb loss.

### TIMS Analytical Technique

The zircon grains were washed in dilute  $\text{HNO}_3$  and rinsed several times in distilled water and acetone in an ultrasonic bath. A mixed  $^{205}\text{Pb}$ - $^{235}\text{U}$  spike was added prior to dissolution in a mixture of HF and  $\text{HNO}_3$  using steel-jacketed Teflon bombs. Chemical separation of Pb and U was done on anion exchange resin using minimal amounts of ultrapure acids. Isotopic analysis was performed on a MAT262 mass spectrometer equipped with an ion counting system. The latter was calibrated by repeated analysis of the NBS 982 standard using the  $^{208}\text{Pb}/^{206}\text{Pb}$  ratio of 1.00016 for mass bias correction (Todt et al., 1996) and second-order nonlinearity calibration of the electron multiplier (Richter et al., 2001). Total procedural Pb blank was estimated at  $0.8 \pm 0.5$  pg. Common Pb in excess of this amount was corrected with the model from Stacey and Kramers (1975) for the respective  $^{206}\text{Pb}/^{238}\text{U}$  age

of the zircon. The uncertainties of the isotopic composition of the spike, blank, and common Pb were taken into account and propagated to the final uncertainties of isotopic ratios and ages. Ages were calculated using ISOPLOT (Ludwig, 2003). U-Pb data are plotted as  $2\sigma$  error ellipses (Fig. 5).

### Determination of Hf Isotopic Composition

The Hf fraction was isolated from the Zr + Hf + rare earth element (REE) fraction of the Pb column chemistry using Eichrom Ln-spec resin and measured in static mode on a NuPlasma multicollector ICP-MS using MCN-6000 and ARIDUS nebulizers for sample introduction. The Hf isotopic values were corrected for a  $^{176}\text{Lu}/^{177}\text{Hf}$  value of 0.0005, typical of zircon. The Hf isotopic ratios were corrected for mass fractionation using a  $^{179}\text{Hf}/^{177}\text{Hf}$  value of 0.7325 and normalized to  $^{176}\text{Hf}/^{177}\text{Hf}$  of 0.28216 of the JMC-475 standard. The isotopic ratios for the chondritic uniform reservoir (CHUR) are those of Blichert-Toft and Albarède (1997).

### Ion-Microprobe Analytical Technique

Zircons were mounted in a resin disk along with the zircon standard and polished to reveal the grain interiors. The mounts were gold-coated and imaged with a Hitachi S-4300 scanning electron microscope (SEM), using a cathodoluminescence probe (CL) to image internal structures, overgrowths, and zonation. Secondary electron mode (SE) imaging was employed to detect fractures and inclusions within the grains. U-Th-Pb zircon analyses (Table DR4, see footnote 1) were performed on a Cameca IMS 1270 ion microprobe following methods described by Whitehouse et al. (1999), which were modified from Whitehouse et al. (1997). U/Pb ratio calibration was based on analyses of the Geostandards zircon 91500, which has an age of  $1065.4 \pm 0.3$  Ma and U and Pb concentrations of 80 and 15 ppm, respectively (Wiedenbeck et al., 1995). Replicate analyses of the same domain within a single zircon were used to independently assess the validity of the calibration. Data reduction employed Excel macros developed by Whitehouse at the Swedish Natural History Museum, Stockholm. Age calculations were made using Isoplot version 3.02 (Ludwig, 2003). U-Pb data are plotted as  $2\sigma$  error ellipses (Fig. 7). All age errors quoted in the text are  $2\sigma$  unless specifically stated otherwise. Common Pb corrections were only applied to samples that exhibited significant levels of  $^{204}\text{Pb}$ , and they are indicated in Table DR4 where applied (see footnote 1). Corrections assume a present-day average terrestrial common Pb composition (Stacey and Kramers, 1975), i.e.,  $^{207}\text{Pb}/^{206}\text{Pb} = 0.83$ . A detailed rationale for choosing present-day Pb as a contaminant is given by Zeck and Whitehouse (1999).

### LA-ICP-MS Analytical Technique

Zircons were mounted in 2.5-cm-diameter epoxy-filled blocks, polished, and cleaned in deionized water and ethanol. Isotopic analysis of zircons by laser-ablation ICP-MS followed the technique described in Kosler et al. (2002). A Thermo-Finnigan Element 2 sector field ICP-MS coupled to a 213 NdYAG laser (New Wave UP-213) at Bergen University was used to measure Pb/U and Pb isotopic ratios in zircons. The sample introduction system was modified to enable simultaneous nebulization of a tracer solution and laser ablation of the solid sample (Horn et al., 2000). Natural  $\text{Ti}$  ( $^{205}\text{Ti}/^{203}\text{Ti} = 2.3871$ ; Dunstan et al., 1980),  $^{209}\text{Bi}$ , and

enriched  $^{233}\text{U}$  and  $^{237}\text{Np}$  (>99%) were used in the tracer solution, which was aspirated to the plasma in an argon-helium carrier gas mixture through an Apex desolvation nebulizer (Elemental Scientific) and a T-piece tube attached to the back end of the plasma torch. A helium gas line carrying the sample from the laser cell to the plasma was also attached to the T-piece tube.

The laser was set up to produce energy density of  $\sim 3\text{ J/cm}^2$  at a repetition rate of 10 Hz. The laser beam was imaged on the surface of the sample placed in the ablation cell, which was mounted on a computer-driven motorized stage of a microscope. During ablation, the stage was moved beneath the stationary laser beam to produce a linear raster ( $\sim 15 \times 50\ \mu\text{m}$ ) in the sample. Typical acquisitions consisted of a 45 s measurement of analytes in the gas blank and aspirated solution, particularly  $^{203}\text{Tl}$ ,  $^{205}\text{Tl}$ ,  $^{209}\text{Bi}$ ,  $^{233}\text{U}$ ,  $^{237}\text{Np}$ , followed by measurement of U and Pb signals from zircon, along with the continuous signal from the aspirated solution, for another 150 s. The data were acquired in time resolved-peak jumping-pulse counting mode with 1 point measured per peak for masses 202 (flyback), 203 and 205 (Tl), 206 and 207 (Pb), 209 (Bi), 233 (U), 237 (Np), 238 (U), 249 ( $^{233}\text{U}$  oxide), 253 ( $^{237}\text{Np}$  oxide), and 254 ( $^{238}\text{U}$  oxide). Raw data were corrected for dead time of the electron multiplier and processed offline in a spreadsheet-based program (Lamdate; Kosler et al., 2002) and plotted on concordia diagrams using IsoPlot (Ludwig, 2003). Data reduction included correction for gas blank, laser-induced elemental fractionation of Pb and U, and instrument mass bias. Minor formation of oxides of U and Np was corrected for by adding signal intensities at masses 249, 253, and 254 to the intensities at masses 233, 237, and 238, respectively. No common Pb correction was applied to the data. Details of data reduction and corrections are described in Kosler et al. (2002) and Kosler and Sylvester (2003). Zircon reference material 91500 (1065 Ma; Wiedenbeck et al., 1995) and an in-house zircon standard (338 Ma; Aftalion et al., 1989) were periodically analyzed during this study.

#### ACKNOWLEDGMENTS

This study was funded by the Swiss National Science Foundation. Use of the NordSIMS was supported by the European Community's program "Structuring the European Research Area" under SYNTHESIS at the Swedish Museum of Natural History, project no. SE-TAF 663. The NordSIMS facility is financed and operated under an agreement between the research councils of Denmark, Norway, and Sweden, the Geological Survey of Finland, and the Swedish Museum of Natural History. We are extremely grateful to J. Macharé, R. Mucho, A. Sanchez, J. Galdos, A. Zapata, S. Carrasco, and R. Mamani of the Geological Survey of Peru (INGEMMET), C. Moreno of San Marcos University in Lima, and Y. Haerberlin and S. Beuchat of the University of Geneva for scientific and logistical support during the field seasons in Peru. The financial and logistical support of L. Seijas and Compania Minera Poderosa S.A. is also gratefully acknowledged. We are very grateful to A. von Quadt for technical assistance with the mass spectrometry at ETH Zürich. The careful and insightful reviews of Ricardo Astini, Robert J. Pankhurst, and Associate Editor Peter Cawood are gratefully acknowledged. This is NordSIMS publication 173.

#### REFERENCES CITED

- Aftalion, M., Bowes, D.R., and Vrána, S., 1989, Early Carboniferous U-Pb zircon age for garnetiferous, perpotassic granulites, Blanský les Massif, Czechoslovakia: *Neues Jahrbuch für Mineralogie-Monatshefte*, v. 4, p. 145–152.
- Astini, R.A., and Davila, F.M., 2004, Ordovician back arc foreland and Ocolyic thrust belt development on the western Gondwana margin as a response to Precordillera terrane accretion: *Tectonics*, v. 23, TC4008, doi: 10.1029/2003TC001620.
- Astini, R.A., Benedetto, J.L., and Vaccari, N.E., 1995, The early Paleozoic evolution of the Argentine Precordillera as a Laurentian rifted, drifted, and collided terrane; a geodynamic model: *Geological Society of America Bulletin*, v. 107, p. 253–273, doi: 10.1130/0016-7606(1995)107<0253:TEPEOT>2.3.CO;2.
- Bahlburg, H., and Hervé, F., 1997, Geodynamic evolution and tectonostratigraphic terranes of northwestern Argentina and northern Chile: *Geological Society of America Bulletin*, v. 109, p. 869–884, doi: 10.1130/0016-7606(1997)109<0869:GEATTO>2.3.CO;2.
- Baldo, E., Casquet, C., Pankhurst, R.J., Galindo, C., Rapela, C.W., Fanning, C.M., Dahlquist, J., and Murra, J., 2006, Neoproterozoic A-type magmatism in the western Sierras Pampeanas (Argentina): Evidence for Rodinia break-up along a proto-Iapetus rift?: *Terra Nova*, v. 18, p. 388–394.
- Bellizija, A., and Pimentel, N., 1994, Terreno Mérida: Un cinturón alóctono Hercínico en la Cordillera de Los Andes de Venezuela: *Sociedad Venezolana de Geólogos, V Simposio Bolivariano Exploración Petrolera en las Cuencas Subandinas, Memoria*, p. 271–299.
- Blichert-Toft, J., and Albarède, F., 1997, The Lu-Hf isotope geochemistry of chondrites and the evolution of the mantle-crust system: *Earth and Planetary Science Letters*, v. 148, p. 243–258, doi: 10.1016/S0012-821X(97)00040-X.
- Boinet, T., Bourgeois, J., Bellon, H., and Toussaint, J.F., 1985, Age et répartition du magmatisme Prémésozoïque des Andes de Colombie: *Comptes Rendus de l'Académie des Sciences de Paris*, v. 300, p. 445–450.
- Caldas, J., 1978, Geología de los Cuadrángulos de San Juan, Acari y Yauca, Hojas: 31-m, 31-n, 32-n: Lima, Instituto Geológico Minero y Metalúrgico, 78 p.
- Cardona, A., Cordani, U., Ruiz, J., Valencia, V., Nutman, A., and Sánchez, A., 2006, U/Pb detrital zircon geochronology and Nd isotopes from Paleozoic metasedimentary rocks of the Marañón Complex: Insights on the proto-Andean tectonic evolution of the Eastern Peruvian Andes: *Fifth South American Symposium on Isotope Geology*, April 24–25 2006, Punta del Este, Uruguay, Short Papers Volume, p. 208–211.
- Cawood, P.A., 2005, Terra Australis orogen: Rodinia breakup and development of the Pacific and Iapetus margins of Gondwana during the Neoproterozoic and Paleozoic: *Earth-Science Reviews*, v. 69, p. 249–279, doi: 10.1016/j.earscirev.2004.09.001.
- Chew, D.M., Schaltegger, U., Mišković, A., Fontignie, D., and Frank, M., 2005, Deciphering the tectonic evolution of the Peruvian segment of the Gondwanan margin, in *Proceedings of the 6th International Symposium on Andean Geodynamics*: Barcelona, Spain, Institut de Recherche pour le Développement, p. 166–169.
- Cordani, U.G., Sato, K., Teixeira, W., Tassinari, C.G., and Basei, M.A.S., 2000, Crustal evolution of the South American Platform, in Cordani, U.G., Milani, E.J., Thomaz-Filho, A., and Campos, D.A., eds., *Tectonic Evolution of South America: Rio de Janeiro, 31st International Geological Congress*, p. 19–40.
- Cordani, U.G., Cardona, A., Jimenez, D.M., Liu, D., and Nutman, A.P., 2005, Geochronology of Proterozoic basement inliers in the Colombian Andes: Tectonic history of remnants of a fragmented Grenville belt, in Vaughan, A.P.M., Leat P.T., and Pankhurst R.J., eds., *Terrane Processes at the Margins of Gondwana: Geological Society of London Special Publication 246*, p. 329–346.
- Dalla Salda, L.H., Dalziel, I.W.D., Cingolani, C.A., and Varela, R., 1992, Did the Taconic Appalachians continue into southern South America?: *Geology*, v. 20, p. 1059–1062, doi: 10.1130/0091-7613(1992)020<1059:DTTACI>2.3.CO;2.
- Dalmayrac, B., Laubacher, G., and Marocco, R., 1980, Géologie des Andes Péruviennes. Caractères Généraux de l'Évolution Géologique des Andes Péruviennes: Paris, Travaux et Document de L'Office de la Recherche Scientifique et Technique Outre-mer, v. 122, 501 p.
- Dalziel, I.W.D., 1991, Pacific margins of Laurentia and East Antarctica—Australia as a conjugate rift pair: Evidence and implications for an Eocambrian supercontinent: *Geology*, v. 19, p. 598–601, doi: 10.1130/0091-7613(1991)019<0598:PMOLAE>2.3.CO;2.
- Dalziel, I.W.D., 1997, Neoproterozoic-Paleozoic geography and tectonics: Review, hypothesis, environmental speculation: *Geological Society of America Bulletin*, v. 109, p. 16–42, doi: 10.1130/0016-7606(1997)109<0016:ONPGAT>2.3.CO;2.
- Dalziel, I.W.D., Dalla Salda, L., and Gahagan, L.M., 1994, Paleozoic Laurentia-Gondwana interaction and the origin of the Appalachian-Andean mountain system: *Geological Society of America Bulletin*, v. 106, p. 243–252, doi: 10.1130/0016-7606(1994)106<0243:PLGIAT>2.3.CO;2.
- Dunstan, L.P., Gramsch, J.W., Barnes, I.L., and Purdy, W.C., 1980, The absolute abundance and the atomic weight of a reference sample of thallium: *Journal of Research of the National Bureau of Standards*, v. 85, p. 1–10.
- Haerberlin, Y., 2002, Geological and structural setting, age, and geochemistry of the orogenic gold deposits at the Patatez Province, eastern Andean Cordillera, Peru [Ph.D. thesis]: Geneva, University of Geneva, 186 p.
- Hoffman, P.F., 1991, Did the breakout of Laurentia turn Gondwanaland inside-out?: *Science*, v. 252, p. 1409–1412, doi: 10.1126/science.252.5011.1409.
- Horn, I., Rudnick, R.L., and McDonough, W.F., 2000, Precise elemental and isotope ratio measurement by simultaneous solution nebulisation and laser ablation-ICP-MS: Application to U-Pb geochronology: *Chemical Geology*, v. 164, p. 281–301, doi: 10.1016/S0009-2541(99)00168-0.
- Kosler, J., and Sylvester, P., 2003, Present trends and the future of zircon in geochronology: *Laser ablation ICPMS: Reviews in Mineralogy & Geochemistry*, v. 53, p. 243–275, doi: 10.2113/0530243.
- Kosler, J., Fonnelland, H., Sylvester, P., Tubrett, M., and Pedersen, R.B., 2002, U-Pb dating of detrital zircons for sediment provenance studies—A comparison of laser ablation ICPMS and SIMS techniques: *Chemical Geology*, v. 182, p. 605–618, doi: 10.1016/S0009-2541(01)00341-2.
- Leon, W., Palacios, O., Vargas, L., and Sanchez, A., 2000, Memoria explicativa del Mapa Geológico del Perú (1999): Lima, Instituto Geológico Minero y Metalúrgico, Carta Geológica Nacional, Boletín No. 136, escala 1:1,000,000.
- Litherland, M., Aspden, J.A., and Jemielita, R.A., 1994, The metamorphic belts of Ecuador: London, British Geological Survey Overseas Memoir 11, 147 p.
- Loewy, S.L., Connelly, J.N., and Dalziel, I.W.D., 2004, An orphaned basement block: The Arequipa-Antofalla basement of the central Andean margin of South America: *Geological Society of America Bulletin*, v. 116, p. 171–187, doi: 10.1130/B25226.1.
- Lork, A., and Bahlburg, H., 1993, Precise U-Pb ages of monazites from the Faja Eruptiva de La Puna Oriental, NW Argentina: Mendoza, XII Congreso Geológico Argentino y II Congreso de Exploración de Hidrocarburos, Actas, v. IV, p. 1–6.
- Lucassen, F., and Becchio, R., 2003, Timing of high-grade metamorphism; early Palaeozoic U-Pb formation ages of titanite indicate long-standing high-*T* conditions at the western margin of Gondwana (Argentina, 26–29°S): *Journal of Metamorphic Geology*, v. 21, p. 649–662, doi: 10.1046/j.1525-1314.2003.00471.x.
- Lucassen, F., and Franz, G., 2005, The early Palaeozoic orogen in the central Andes: A non-collisional orogen comparable to the Cenozoic high plateau?, in Vaughan, A.P.M., Leat P.T., and Pankhurst R.J., eds., *Terrane Processes at the Margins of Gondwana: Geological Society of London Special Publication 246*, p. 257–274.
- Ludwig, K.R., 1998, On the treatment of concordant uranium-lead ages: *Geochimica et Cosmochimica Acta*, v. 62, p. 665–676, doi: 10.1016/S0016-7037(98)00059-3.
- Ludwig, K.R., 2003, User's Manual for Isoplot 3.00. A Geochronological Toolkit for Microsoft Excel: Berkeley Geochronology Center Special Publication 4, 56 p.
- Macfarlane, A., 1999, Isotopic studies of northern Andean crustal evolution and ore metal sources, in Skinner, B.J., ed., *Geology and Ore Deposits of the Central*

- Andes: Boulder, Society of Economic Geologists, v. 7, p. 195–217.
- Marechal, P., 1983, Les temoins de chaîne Hercynienne dans le noyau ancien des Andes de Mérida (Vénézuéla). Structure et evolution tectonometamorphique [Ph.D. thesis]: Brest, University of Brest, 180 p.
- Meert, J.G., and Torsvik, T.H., 2003, The making and unmaking of a supercontinent: Rodinia revisited: *Tectonophysics*, v. 375, p. 261–288, doi: 10.1016/S0040-1951(03)00342-1.
- Mégard, F., 1978, Etude Géologique des Andes du Peru Central: Paris, Travaux et Document de L'Office de la Recherche Scientifique et Technique Outre-mer, v. 86, 310 p.
- Mišković, A., Schaltegger, U., and Chew, D.M., 2005, Carboniferous plutonism along the Eastern Peruvian Cordillera: Implications for the late Paleozoic to early Mesozoic Gondwanan tectonics, in *Proceedings of the 6th International Symposium on Andean Geodynamics*, Barcelona, Spain, Institut de Recherche pour le Développement, p. 508–511.
- Mukasa, S.B., and Henry, D.J., 1990, The San Nicolas Batholith of coastal Peru; early Palaeozoic continental arc or continental rift magmatism?: *Journal of the Geological Society of London*, v. 147, p. 27–39.
- Omarini, R.H., Sureda, R.J., Goetze, H.J., Seilacher, A., and Pflueger, F., 1999, Puncoviscana folded belt in northwestern Argentina; testimony of late Proterozoic Rodinia fragmentation and pre-Gondwana collisional episodes: *International Journal of Earth Sciences*, v. 88, p. 76–97, doi: 10.1007/s005310050247.
- Pankhurst, R.J., Rapela, C.W., Saavedra, J., Baldo, E., Dahquist, J., Pascua, I., and Fanning, C.M., 1998, The Famatinian magmatic arc in the central Sierras Pampeanas: An Early to Mid-Ordovician continental arc on the Gondwana margin, in Pankhurst, R.J., and Rapela, C.W., eds., *The Proto-Andean Margin of Gondwana*: Geological Society of London Special Publication 142, p. 343–367.
- Pankhurst, R.J., Rapela, C.W., and Fanning, C.M., 2000, Age and origin of coeval TTG, I- and S-type granites in the Famatinian belt of NW Argentina: *Transactions of the Royal Society of Edinburgh, Earth Sciences*, v. 91, p. 151–168.
- Pankhurst, R.J., Rapela, C.W., Fanning, C.M., and Márquez, M., 2006, Gondwanide continental collision and the origin of Patagonia: *Earth-Science Reviews*, v. 76, p. 235–257, doi: 10.1016/j.earscirev.2006.02.001.
- Pimentel, M.M., Fuck, R.A., and Botelho, N.F., 1999, Granites and the geodynamic history of the Neoproterozoic Brasília belt, central Brazil: a review: *Lithos*, v. 46, p. 463–483, doi: 10.1016/S0024-4937(98)00078-4.
- Pisarevsky, S.A., Wingate, M.T.D., Powell, C.M., Johnson, S., and Evans, D.A.D., 2003, Models of Rodinia assembly and fragmentation, in Yoshida, M., Windley, B.F., and Dasgupta, S., eds., *Proterozoic East Gondwana: Supercontinent Assembly and Breakup*: Geological Society of London Special Publication 206, p. 35–55.
- Polliand, M., Schaltegger, U., Frank, M., and Fontboté, L., 2005, Formation of intra-arc volcanosedimentary basins in the western flank of the central Peruvian Andes during Late Cretaceous oblique subduction; field evidence and constraints from U-Pb ages and Hf isotopes: *International Journal of Earth Sciences*, v. 94, p. 231–242, doi: 10.1007/s00531-005-0464-5.
- Pratt, W.T., Duque, P., and Ponce, M., 2005, An autochthonous geological model for the eastern Andes of Ecuador: *Tectonophysics*, v. 399, p. 251–278, doi: 10.1016/j.tecto.2004.12.025.
- Pupin, J.P., 1980, Zircon and granite petrology: *Contributions to Mineralogy and Petrology*, v. 73, p. 207–220, doi: 10.1007/BF00381441.
- Ramos, V.A., and Aleman, A., 2000, Tectonic evolution of the Andes, in Cordani, U., Milani, E.J., Thomaz Filho, A., and Campos Neto, M.C., eds., *Tectonic Evolution of South America*: Rio de Janeiro, Institut de Recherche pour le Développement, p. 635–685.
- Ramos, V.A., Jordan, T.E., Allmendinger, R.W., Mpodozis, M.C., Kay, S.M., Cortes, J.M., and Palma, M., 1986, Paleozoic terranes of the central Argentine-Chilean Andes: *Tectonics*, v. 5, p. 855–880.
- Rapela, C.W., Pankhurst, R.J., Casquet, C., Baldo, E., Saavedra, J., and Galindo, C., 1998, Early evolution of the proto-Andean margin of South America: *Geology*, v. 26, p. 707–710, doi: 10.1130/0091-7613(1998)026<0707:EEOTPA>2.3.CO;2.
- Restrepo-Pace, P.A., Ruiz, J., Gehrels, G., and Cosca, M., 1997, Geochronology and Nd isotopic data of Grenville-age rocks in the Colombian Andes: New constraints for late Proterozoic–early Paleozoic paleocontinental reconstructions of the Americas: *Earth and Planetary Science Letters*, v. 150, p. 427–441.
- Richter, S., Goldberg, S.A., Mason, P.B., Traina, A.J., and Schwieters, J.B., 2001, Linearity tests for secondary electron multipliers used in isotope ratio mass spectrometry: *International Journal of Mass Spectrometry*, v. 206, p. 105–127.
- Sanchez, A., 1983, Nuevos datos K-Ar en algunas rocas del Perú: *Boletín Sociedad Geológica del Perú*, v. 71, p. 193–202.
- Santos, J.O., Easton, R.M., Potter, P.E., Rizzotto, G.A., Hartmann, L.A., and McNaughton, N.J., 2002, The Sunsas orogen in western Amazon Craton, South America, and correlation with the Grenville orogen of Laurentia, based on U-Pb isotopic study of detrital and igneous zircons: *Geological Society of America Abstracts with Programs*, v. 34, no. 6, p. 272.
- Stacey, J.S., and Kramers, J.D., 1975, Approximation of terrestrial lead isotope evolution by a 2-stage model: *Earth and Planetary Science Letters*, v. 26, p. 207–221, doi: 10.1016/0012-821X(75)90088-6.
- Steinmann, G., 1929, *Geologie von Peru*: Heidelberg, Germany, Carl Winters Universitätsbuchhandlung, 448 p.
- Thomas, W.A., and Astini, R.A., 2003, Ordovician accretion of the Argentine Precordillera terrane to Gondwana: A review: *Journal of South American Earth Sciences*, v. 16, p. 67–79, doi: 10.1016/S0895-9811(03)00019-1.
- Thomas, W.A., Astini, R.A., and Bayona, G., 2002, Ordovician collision of the Argentine Precordillera with Gondwana, independent of Laurentian Taconic orogeny: *Tectonophysics*, v. 345, p. 131–152.
- Thomas, W.A., Astini, R.A., Mueller, P.A., Gehrels, G.E., and Wooden, J.L., 2004, Transfer of the Argentine Precordillera terrane from Laurentia: Constraints from detrital-zircon geochronology: *Geology*, v. 32, p. 965–968, doi: 10.1130/G20727.1.
- Todt, W., Cliff, R.A., Hanser, A., and Hofmann, A.W., 1996, Evaluation of a <sup>202</sup>Pb-<sup>203</sup>Pb double spike for high-precision lead isotopic analyses, in Basu, A., and Hart, S., eds., *Earth Processes: Reading the Isotopic Code*: American Geophysical Union Geophysical Monograph 95, p. 429–437.
- Wasteneys, H.A., Clark, A.H., Farrar, E., and Langridge, R.J., 1995, Grenvillian granulite-facies metamorphism in the Arequipa Massif, Peru; a Laurentia-Gondwana link: *Earth and Planetary Science Letters*, v. 132, p. 63–73, doi: 10.1016/0012-821X(95)00055-H.
- Whitehouse, M.J., Claesson, S., Sunde, T., and Vestin, J., 1997, Ion microprobe U-Pb zircon geochronology and correlation of Archaean gneisses from the Lewisian Complex of Grinnard Bay, northwestern Scotland: *Geochimica et Cosmochimica Acta*, v. 61, p. 4429–4438, doi: 10.1016/S0016-7037(97)00251-2.
- Whitehouse, M.J., Kamber, B.S., and Moorbath, S., 1999, Age significance of U-Th-Pb zircon data from Early Archaean rocks of west Greenland: A reassessment based on combined ion-microprobe and imaging studies: *Chemical Geology*, v. 160, p. 201–224, doi: 10.1016/S0009-2541(99)00066-2.
- Wiedenbeck, M., Allé, P., Corfu, F., Griffin, W., Meier, M., Oberli, F., von Quadt, A., Roddick, J.C., and Spiegel, W., 1995, Three natural zircon standards for U-Th-Pb, Lu-Hf, trace element and REE analysis: *Geostandards Newsletter*, v. 19, p. 1–23.
- Wilson, J., and Reyes, L., 1964, *Geología del Cuadrángulo de Pataz*: Lima, Instituto Geológico Minero y Metalúrgico, Carta Geológica Nacional, Boletín Serie A, v. 9, 91 p., scale 1:100,000.
- Wilson, J., Reyes, L., and Garayar, J., 1995, *Geología de los Cuadrángulos de Pallasca, Tayabamba, Corongo, Pomabamba, Carhuaz y Huari*: Lima, Instituto Geológico Minero y Metalúrgico, Carta Geológica Nacional, Boletín Serie A, v. 60, 63 p., scale 1:100,000.
- Zeck, H.P., and Whitehouse, M.J., 1999, Hercynian, Pan-African, Proterozoic and Archaean ion microprobe zircon ages for a Betic-Rif core complex, Alpine belt, W. Mediterranean consequences for its *P–T–t* path: *Contributions to Mineralogy and Petrology*, v. 134, p. 134–149, doi: 10.1007/s004100050474.
- Zeck, H.P., Wingate, M.T.D., Pooley, G.D., and Ugidos, J.M., 2004, A sequence of Pan-African Hercynian events recorded in zircons from an orthogneiss from the Hercynian belt of western central Iberia: an ion microprobe U-Pb study: *Journal of Petrology*, v. 45, p. 1613–1629, doi: 10.1093/petrology/egh026.

MANUSCRIPT RECEIVED 24 JULY 2006  
 REVISED MANUSCRIPT RECEIVED 16 OCTOBER 2006  
 MANUSCRIPT ACCEPTED 19 NOVEMBER 2006

Printed in the USA